THE INITIAL DENSITY DEPENDENCE OF THE DIFFUSION COEFFICIENT FOR BINARY GAS SYSTEMS

by

IAN ROBERT SHANKLAND, B. Sc. (Hons.)

A THESIS SUBMITTED FOR THE DEGREE OF

DOCTOR OF PHILOSOPHY

AT THE UNIVERSITY OF ADELAIDE,

MARCH, 1979.

Awarded October 1979

DEPARTMENT OF PHYSICAL AND INORGANIC CHEMISTRY

ERRATA

page 12	line 5	"nolecules" should read "molecules".
page 13	line 12	"expressions" should read "expression".
page 23	line 20	interchange "upper" and "lower"
page 90		Equation (7.5) should be the same as Equation (I.8), page 108.
page 93		Equation below (7.12) should be numbered (7.13).
page 111		Table title, "3000.00" should read "300.00".

Substitute Z for z in equations (6.12), (I.17), (I.18), (I.20).

ABSTRACT

Binary diffusion coefficients have been determined at 300.00 and 323.16 K over the pressure range 1 - 25 atmospheres for the systems N_2 + Ar, N_2 + O_2 and O_2 + Ar. Similar data is reported for the Ar + Kr system to a maximum pressure of 10 atmospheres.

These results were obtained via the classical Loschmidt technique; a mass spectrometric procedure being employed for concentration measurements. To attain the greatest degree of accuracy only systems with small excess thermodynamic properties were studied. An analysis of possible sources of error is given and where possible numerical estimations are made.

A comparison of diffusion data obtained with the classical Loschmidt technique and another method, developed previously in this laboratory, is described. Concordance between both methods is excellent.

The density dependence of the diffusion coefficient is discussed with reference to the Enskog-Thorne result for rigid spherical molecules. Poor agreement between the experimental and predicted first density corrections was observed. No improvement was achieved through the empirical modification of the Enskog theory.

I declare that this thesis contains no material accepted for any degree or diploma in any university or institution and that, to the best of my knowledge and belief, it contains no material previously published or written by any other person, except where due reference is made in the text.

I.R. Shankland.

ACKNOWLEDGEMENTS

It is a pleasure to acknowledge the tireless enthusiasm and encouragement of Dr. Peter J. Dunlop under whose guidance this work was performed.

My appreciation also goes to my colleagues in the Department for their interest in this work and to the members of the technical staff for their assistance in the construction of the experimental apparatus.

I am indebted once again to Dr. Peter J. Dunlop for his constructive criticism of the original draft, to Mr. Andrew B. Miller for the salvation of my syntax, and to Mrs. Angela McKay for her expertise in the typing of this thesis. Finally, to my wife Erica whose ability to check endless tables of numerical data is only exceeded by her patience and understanding.

This work was completed under the tenure of a Commonwealth Postgraduate Award.

TABLE OF CONTENTS

LIST OF TABLES

LIST OF FIGURES

CHAPTER I

INTRODUCTION

Over the past few decades numerous comparisons have been made between theoretical results concerning the density dependence of transport properties and the experimentally observed dependence. To a large extent these comparisons have involved the coefficients of viscosity and thermal conductivity[1-8]. In contrast, there exists a scarcity of accurate diffusion measurements which can be employed for similar purposes. Of the data available, the majority pertain to measurements of *tracer diffusion coefficients*[9-19]; in particular, the diffusion of radioactive tracers into the isotopically normal gases[9-16] has been studied over a wide range of pressures as an approximate means of determining the density dependence of self-diffusion. For the case of diffusion in binary systems at concentrations other than trace amounts, such data are even more rare; Sage and co-workers[20,21] have published diffusion coefficients for $CH_4 + n - C_7H_{16}$, Berry and Koeller[22] for $H_2 + N_2$, $CH_4 + C_2H_6$, $CH_4 + N_2$ and $N_2 + C_2H_6$, Islam and Stryland[23] for CH_4 + Ar, and De Paz *et al.*[24] for the He + Ar and Ne + Ar systems. However, the accuracy of these results is probably no better than ±5%.

More recently Staker and Dunlop[25], and Bell *et al.*[26] have reported binary diffusion data at 300K for sixteen gaseous systems containing approximately 90% helium. Although the

maximum pressure at which measurements were performed was only 9 atmospheres, important information concerning the *initial* density dependence was obtained. Arora and Dunlop[27] have since extended this work for the systems He + Ar, He + N_2, He + O_2 and He + CO_2 to pressures in the region of 20 atmospheres and to a temperature of 323K. The experimental technique used for these measurements[28] was developed in this laboratory and consists basically of monitoring the concentration difference in a Loschmidt-type diffusion cell[25] with a precision thermistor bridge[29]. However, as this technique has proved unsuccessful at elevated pressures for systems which do not contain excess helium[25], a different experimental approach was employed in this study.

The method adopted still involved the use of a similar type of cell, but is based on Loschmidt's[30] original mathematical analysis. In this case concentrations need only be determined once, after an initial diffusion period; such determinations were accomplished via the use of a mass spectrometer. Details of the relevant theory and experimental procedures are outlined in Chapters III, IV and V. To achieve optimum accuracy in the measured diffusion coefficients it was necessary to restrict the systems studied to those which possessed small excess thermodynamic properties. In Chapters III and VI this limitation is shown to be especially important at increased densities. Results obtained with the classical Loschmidt and thermistor bridge techniques are compared in Chapter VI.

Binary diffusion data for the systems N_2 + Ar, N_2 + O_2, O_2 + Ar and Ar + Kr, to a maximum pressure of 25 atmospheres

and at temperatures of 300 and 323K, are reported in the final chapter. These results are discussed in terms of the Enskog theory[31] of rigid spheres.

REFERENCES

1. J.V. Sengers, Int. J. *Heat Mass Transfer* 8 1103 (1965).

2. H.J.M. Hanley, R.D. McCarty and J.V. Sengers, *J. Chem. Phys.* 50 857 (1969).

3. J.A. Gracki, G.P. Flynn and J. Ross, *ibid.* 51 3856 (1969).

4. J. Kestin, E. Paykoc and J.V. Sengers, *Physica* 54 1 (1971).

5. H.J.M. Hanley, R.D. McCarty and E.G.D. Cohen, *ibid.* 60 322 (1972).

6. J.F. Ely and D.A. McQuarrie, *J. Chem. Phys.* 60 4105 (1974).

7. W.A. Wakeham, J. Kestin, E.A. Mason and S.I. Sandler, *ibid.* 57 295 (1972).

8. R. Di Pippo, J.R. Dorfman, J. Kestin, H.E. Khalifa and E.A. Mason, *Physica* 86A 205 (1977).

9. K.D. Timmerhaus and H.G. Drickamer, *J. Chem Phys.* 19 1242 (1951); 20 981 (1952).

10. W.L. Robb and H.G. Drickamer, *ibid.* 19 1504 (1951).

11. Q.R. Jeffries and H.G. Drickamer, *ibid.* 21 1358 (1953).

12. E. Becker, W. Vogell and F. Zigan, *Z. Naturforsch.* 8a 686 (1953).

13. H.A. O'Hern Jr. and J.J. Martin, *Ind. Eng. Chem.* 47 2081 (1955).

14. L. Durbin and R. Kobayashi, *J. Chem. Phys.* 37 1643 (1962).

15. N.J. Trappeniers and J.P.J. Michels, *Chem. Phys. Letters* 18 1 (1972).

16. P. Codastefano, M.A. Ricci and V. Zanza, *Physica* 92A 315 (1978).

17. Q.R. Jeffries and H.G. Drickamer, *J. Chem. Phys.* 22 436 (1954).

18. C. Chou and J.J. Martin, *Ind. Eng. Chem.* 49 758 (1957).

19. Z. Balenovic, M.N. Myers and J.C. Giddings, *J. Chem. Phys.* 52 915 (1970).

20. L.T. Carmichael, B.H. Sage and W.N. Lacey, *A. I. Ch. E. Journal* 1 385 (1955).

21. H.H. Reamer and B.H. Sage, *J. Chem. Eng. Data* 8 34 (1963).

22. V.J. Berry Jr. amd R.C. Koeller, *A. I. Ch. E. Journal* 6 274 (1960).

23. M. Islam and J.C. Stryland, *Physica* 45 115 (1969).

24. M. De Paz, F. Tantalo and G. Varni, *J. Chem. Phys.* 61 3875 (1974).

25. G.R. Staker and P.J. Dunlop, *Chem. Phys. Letters* 42 419 (1976).

26. T.N. Bell, I.R. Shankland and P.J. Dunlop, *ibid.* 45 445 (1977).

27. P.S. Arora and P.J. Dunlop, to be published.

28. P.J. Carson, P.J. Dunlop and T.N. Bell, *J. Chem. Phys.* 56 531 (1972).

29. M.A. Yabsley and P.J. Dunlop, *J. Phys. E: Sci. Instrum.* 8 834 (1975).

30. J. Loschmidt, *Akad. Wiss. Wien* 61 367 (1870).

31. S. Chapman and T.G. Cowling, *The Mathematical Theory of Non-uniforn Gases*, Cambridge University Press, 3rd edition (1970).

CHAPTER II

THE KINETIC THEORY OF GASES

2.1 Chapman-Enskog Theory of Dilute Gases

Calculation of transport properties from molecular theory is most convenient for dilute gases composed of monatomic particles. The rigorous kinetic theory of such systems was developed independently by Chapman and Enskog[1]. Since their treatment is rather involved and lengthy, only a brief description of the basic assumptions and the results for binary diffusion are given here.

The Chapman-Enskog theory is centred upon the procurement of a solution for the single particle or first order distribution function $f_i(\underset{\sim}{r}, \underset{\sim}{v}_i, t)$; this distribution function is defined so that $f_i(\underset{\sim}{r}, \underset{\sim}{v}_i, t)d\underset{\sim}{r}\, d\underset{\sim}{v}_i$ is the probable number of molecules of kind i with spatial coordinates in the range $d\underset{\sim}{r}$ about $\underset{\sim}{r}$ and velocities in the range $d\underset{\sim}{v}_i$ about $\underset{\sim}{v}_i$ at time t. A complete description of a dilute gas can be obtained by relating the macroscopic fluxes through velocity averages to the distribution function.

In order to determine f_i, the Boltzmann integro-differential equation, which describes the variation of f_i due to molecular interactions, must be solved. The Chapman-Enskog approach to the solution of the Boltzmann equation is essentially a perturbation method which involves expanding f_i in a series about the equilibrium distribution,

$$f_i = f_i^{(0)} + f_i^{(1)} + f_i^{(2)} + \ldots \quad . \qquad (2.1)$$

The first term, $f_i^{(0)}$, is simply the Maxwell-Boltzmann equilibrium distribution function. When the expansion (2.1) is truncated after the first correction term and substituted into the Boltzmann equation, a linearised integro-differential equation for $f_i^{(1)}$ results. The perturbation is assumed proportional to the relevant transport gradient and solved for by further expansions in terms of the molecular velocities[1,2]. Finally, the transport coefficients can be expressed as a ratio of two infinite determinants[1] which in general cannot be solved exactly. However, numerical values for the coefficients may be obtained by systematically truncating the determinants. Two such approximation schemes in common usage are the method of Chapman and Cowling[1] and that of Kihara[3]. The simplest truncation gives rise to the first approximation of the transport coefficient, the next gives the second approximation and so on.

The major assumptions inherent in the Chapman-Enskog theory can be summarised as:-

(i) *Molecular chaos.*

In the derivation of the Boltzmann equation from the Liouville equation[2] it is necessary to assume that for two particles prior to collision, and far enough apart for molecular interactions to be ignored, there are no correlations between $\underset{\sim}{v}_1$ and $\underset{\sim}{v}_2$ or between $\underset{\sim}{r}_1$ and $\underset{\sim}{r}_2$. This permits the second order distribution function to be expressed as the product of the two first order functions and hence a closed equation is produced.

(ii) *Binary collisions.*

Again this assumption is inherent in the Boltzmann equation and means that the results do not apply where ternary and higher order collisions occur. Therefore the theory is limited to dilute gases.

(iii) *Small molecular size.*

If the molecular dimensions are negligible when compared with the mean free path, then the distribution functions, f_1 and f_2, for the colliding molecules 1 and 2 can be evaluated at the same point $\underset{\sim}{r}$ in space.

(iv) *Small mean free path.*

When the dimensions of the gas container are large in comparison to the mean free path, collisions with the container walls can be neglected. At very low pressures collisions with the walls predominate over intermolecular collisions and the theory is in error.

(v) *Small perturbations.*

The assumption of proportionality between the transport fluxes and gradients is only valid for small departures from equilibrium. Under more extreme conditions, for example shock waves, the third and higher terms of Equation (2.1) may have to be considered.

(vi) *Elastic collisions.*

The theory is strictly pertinent to monatomic molecules. Where molecules possess internal degrees of freedom, kinetic energy may not be conserved during collisions. However, as this does not greatly affect diffusion, the theory can be applied to simple polyatomic molecules.

(vii) *Classical mechanics.*

The use of classical mechanics by Chapman and Enskog restricts the theory to those situations where quantum effects can be neglected. Quantum mechanical modifications of the theory[1,2] are generally unimportant except where hydrogen or helium are involved.

The failure of some of these assumptions at increased pressures is discussed in the next section.

For a binary gas mixture the Chapman-Enskog result for the diffusion coefficient, D_{12}, is to a first approximation

$$n[D_{12}]_1 = \frac{3}{8}(kT/2\pi\mu_{12})^{1/2}/\sigma_{12}^2\,\Omega_{12}^{(1,1)*}(T_{12}^*). \qquad (2.2)$$

Here n denotes the number density of the mixture, T the absolute temperature and $\mu_{12} = m_1 m_2/(m_1+m_2)$ the reduced molecular mass. The reduced collision integral, $\Omega_{12}^{(1,1)*}$, is a function of the reduced temperature $T_{12}^* = kT/\varepsilon_{12}$ where ε_{12} is the depth of the potential energy well; $\Omega_{12}^{(1,1)*}$ is dependent upon the form of the intermolecular potential function through the dynamics of a binary molecular collision. Thus, a knowledge of the intermolecular potential function permits calculation of the diffusion coefficient or *vice versa*, measurements of the diffusion coefficient may yield information concerning the potential function. The intermolecular distance at which the interaction energy is zero is denoted by σ_{12}. Tabulations of $\Omega_{12}^{(1,1)*}$ versus T_{12}^* have been performed[4] for a variety of potential functions.

At the first approximation, the diffusion coefficient is independent of composition and inversely proportional to the number density. The former relation is changed with the introduction of the higher approximations which may be expressed in the form

$$[D_{12}]_k = [D_{12}]_1 \; f_D^{(k)} \quad , \tag{2.3}$$

where k represents the degree of approximation. The Chapman-Cowling second approximation may be written as

$$f_D^{(2)} = 1/(1 - \Delta_{12}) , \tag{2.4}$$

where Δ_{12} is a function of molefractions, molecular masses, molecular sizes and collision integrals; the Kihara expression is of the form

$$f_D^{(2)} = 1 + \Delta'_{12} \quad . \tag{2.5}$$

Explicit formulae for Δ_{12} and Δ'_{12} can be found in most relevant texts[1,2].

The relationship between $[D_{12}]_k$ and the experimentally determined mutual diffusion coefficient $\mathcal{D}_{12}$, which is defined in the next chapter, is

$$\mathcal{D}_{12} = \lim_{k \to \infty} [D_{12}]_k \quad . \tag{2.6}$$

Fortunately convergence of the approximation scheme is rapid with the third and higher approximations being almost identical. At moderate densities, Equation (2.6) is complicated by the real nature of the gas systems and is considered further in the next section.

2.2 *The Enskog Extension to Moderately Dense Gases*

The first rigorous attempt at describing the density dependence of transport properties was due to Enskog[1] who considered an hypothetical gas composed of rigid spherical nolecules with diameter σ . This model permits the mathematical simplifications arising from the neglection of ternary and higher order collisions[1,5] . Of the other assumptions fundamental to the dilute gas theory only (i) and (iii) (see §2.1) need reconsideration at moderate densities.

When gases are compressed the molecular size becomes comparable with the average intermolecular separation and assumption (iii) is invalidated. The finite size of molecules has two effects, firstly, the collision frequency is altered and secondly, there is a transfer of momentum and energy across the finite distance which separates the centres of the molecules during collision. However, as there is no transfer of mass during collision the latter phenomenon is unimportant in diffusion. To account for these effects, Enskog incorporated in the Boltzmann equation a quantity Y, representing the factor by which the collision frequency differed from that of a gas composed of point particles. Furthermore, the distribution functions of the colliding molecules were distinguished by a distance σ in contrast with assumption (iii).

The factor Y is identified with the *equilibrium* radial distribution function for rigid spheres, evaluated at an intermolecular distance of σ . In this manner correlations between molecular positions were assumed identical to the equilibrium situation[5,6] ; however, the molecular chaos

assumption was retained for velocities. The equation of state for a single component rigid sphere gas is related to Y through

$$P = nkT(1 + \frac{2}{3}\pi n\sigma^3 Y). \tag{2.7}$$

For self-diffusion, the Enskog solution of the modified Boltzmann equation yields

$$nD = (nD)_0/Y \ , \tag{2.8}$$

where $(nD)_0$ is the low density value and Y is defined by

$$Y = 1 + \frac{5}{12}\, n\pi\sigma^3 + \ldots \ . \tag{2.9}$$

This result has been extended to binary mixtures by Thorne[1] and to multicomponent mixtures by Tham and Gubbins[7]. Thorne's expressions for the binary diffusion coefficient is given by

$$nD_{12} = (nD_{12})_0/Y_{12} \ , \tag{2.10}$$

with

$$Y_{12} = 1 + \frac{2}{3}\, n\pi\left[x_1 \sigma_{11}^3\left(\frac{\sigma_{11}+4\sigma_{22}}{4\sigma_{11}+4\sigma_{22}}\right) + x_2\sigma_{22}^3\left(\frac{4\sigma_{11}+\sigma_{22}}{4\sigma_{11}+4\sigma_{22}}\right)\right] + \ldots \ . \tag{2.11}$$

In order that Equation (2.10) can be employed for comparison with experimental data, the Thorne diffusion coefficient, D_{12}, must be related to the measured quantity $\mathcal{D}_{12}$. The required relation being[7]

$$(n\mathcal{D}_{12})/(nD_{12}) = (\partial \ell n a_1/\partial \ell n x_1)_{T,P} \ , \tag{2.12}$$

where a_1 is the activity of component 1. An expression for $(\partial \ell n a_1/\partial \ell n x_1)_{T,P}$ is given in Appendix I. Combination of Equations (2.10) and (2.12) gives

$$(n\mathcal{D}_{12})/(n\mathcal{D}_{12})_0 = Y_{12}^{-1}(\partial \ell n a_1/\partial \ell n x_1)_{T,P} \quad . \qquad (2.13)$$

Expansion of this equation as a series in n yields

$$(n\mathcal{D}_{12})/(n\mathcal{D}_{12})_0 = 1 + B_D n + C_D n^2 + \ldots \quad , \qquad (2.14)$$

where B_D and C_D are termed the first and second density corrections to the dilute gas diffusion coefficient; the first density correction is considered further in Chapter VII.

Recent considerations[8-10] of the Enskog-Thorne results have shown that they are inconsistent with the Onsager reciprocal relations. However, such discrepancies do not affect the first density correction for isothermal diffusion. Van Beijeren and Ernst[10] have reformulated the theory in terms of a local-equilibrium radial distribution function which accounts for spatial non-uniformities in the local number density. The modified theory is consistent with the Onsager reciprocal relations.

2.3 Rigorous Kinetic Theory of Dense Gases

A more general statistical mechanical theory of dense gases[11] has been developed from a set of integro-differential equations obtained by integration of the Liouville equation. This set of equations is known as the BBGKY hierachy after Born, Bogoliubov, Green, Kirkwood and Yvon; the first equation involves the first and second order distribution functions and is similar in form to the Boltzmann equation. The theory implies an expansion series, analogous to Equation (2.14), for the transport coefficients. Successively higher order events occurring between molecules determine the coefficients of the

series. Because of the mathematical difficulties encountered, exact formulae for the transport properties have proved impossible to obtain without making approximations.

Curtiss and co-workers[12,13] retained some of the Enskog assumptions and derived expressions for the first density corrections. Their treatment included the effects of collisional transfer and three-body collisions for gases obeying an arbitrary potential; effects due to bound pairs of molecules were not considered. As the necessary integrations[13] have not been performed for binary systems, these results could not be compared with the data obtained in this study.

In a gas at high density, sequences of correlated collisions can occur and hence molecular velocities may be correlated over distances greater than the distance of molecular interaction. Such deviations from molecular chaos cause divergence[14-16] in some coefficients of the density expansion. The expansion for a transport property, α , then takes the form

$$\alpha/\alpha_0 = 1 + B_\alpha \rho + C'_\alpha \rho^2 + C''_\alpha \rho^2 \ell n \rho + \ldots , \qquad (2.15)$$

where $\rho = na^3$ and a is the molecular diameter. Various attempts[6,17,18] at fitting experimental data to an equation of this type have been made, but no substantiative evidence for the inclusion of the logarithmic term has been obtained. As the diffusion coefficients measured in this work could be adequately described by an equation linear in n , Equation (2.15) is considered no further.

REFERENCES

1. S. Chapman and T.G. Cowling, *The Mathematical Theory of Non-uniform Gases*, 3rd. edition, Cambridge University Press (1970).

2. J.O. Hirschfelder, C.F. Curtiss and R.B. Bird, *Molecular Theory of Gases and Liquids*, 4th. printing, Wiley (1967).

3. E.A. Mason, *J. Chem. Phys.* 27 75, 782 (1957).

4. See for example, M. Klein, H.J.M. Hanley, F.J. Smith and P. Holland, *Tables of Collision Integrals and Second Virial Coefficients for the (m,6,8) Intermolecular Potential Function*, U.S. National Bureau of Standards Circular, NSRD - NBS47 (1974).

5. T.M. Reed and K.E. Gubbins, *Applied Statistical Mechanics*, McGraw-Hill (1973).

6. J. Kestin, E. Paykoc and J.V. Sengers, *Physica* 54 1 (1971).

7. M.K. Tham and K.E. Gubbins, *J. Chem. Phys.* 55 268 (1971).

8. L.S. Garcia-Colin, L. Barajas and E. Piña, *Phys. Letters* 37A 395 (1971).

9. L. Barajas, L.S. Garcia-Colin and E. Piña, *J. Stat. Phys.* 7 161 (1971).

10. H. Van Beijeren and M.H. Ernst, *Physica* 68 437 (1973); 70 225 (1973).

11. See for example, S.G. Brush, *Kinetic Theory*, Vol. 3, Pergamon Press (1972) and reference 1.

12. D.K. Hoffmann and C.F. Curtiss, *Phys. Fluids* 8 890 (1965), and references cited therein.

13. D.E. Bennett III and C.F. Curtiss, *J. Chem. Phys.* 51 2811 (1969).

14. J.R. Dorfman and E.G.D. Cohen, *J. Math. Phys.* 8 282 (1967).

15. K. Kawasaki and I. Oppenheim, *Phys. Rev.* 139 A1763 (1965).

16. Y. Kan and J.R. Dorfman, *Phys. Rev. A* 16 2447 (1977).

17. J.A. Gracki, G.P. Flynn and J. Ross, *J. Chem. Phys.* 51 3856 (1969).

18. H.J.M. Hanley, R.D. McCarty and J.V. Sengers, *ibid.* 50 857 (1969).

CHAPTER III

BASIS OF EXPERIMENTAL METHOD

3.1 Introduction

Diffusion may be defined as that process whereby a *relative flow* of components is caused by the presence of a potential gradient. While this gradient may manifest itself in a variety of forms, that which arises solely from a difference in concentration is of interest here. This type of diffusion is termed *ordinary diffusion.*

Although diffusion is generally a three-dimensional process, the present discussion is simplified by considering the flow of matter in a single dimension. Because the relationships between the component fluxes and the concentration gradients causing them are of central importance in any experimental observation of diffusion, a brief outline of the major *flow equations* is given below. This discussion is strictly pertinent to those systems where isothermal conditions exist. However, it must be realised that the transport of matter produces a flow of energy and thus temperature gradients; this phenomenon is known as the Dufour effect[1] and its consequences will be neglected for the moment.

3.2 *Flow Equations and Frames of Reference*

Most mathematical analyses of diffusion experiments begin with the statement that the rate of mass transfer is proportional to the relevant concentration gradient. This was first formulated by Fick[2] in 1855 and is generally known as Fick's first law of diffusion. In order to make use of this law in a definitive manner, it is necessary to specify a *frame of reference* in which measurements can be based and also to show that Fick's law is applicable in this frame. Experimental observations are commonly based on a reference frame defined by the diffusion cell[3] whereas the phenomenological flow equations[4,5] are discussed in terms of more general reference frames. Specifically the *volume-fixed* frame, defined as that reference frame moving with the same velocity as the *local* centre of volume, is of importance[5,6] in experimental situations.

If the local flux of component i in a binary system is denoted by J_i and defined as the number of moles of i crossing unit area normal to the direction of diffusion in unit time, then the relationship between the fluxes in the volume-fixed frame is

$$\sum_{i=1}^{2} \bar{V}_i (J_i)_V = 0. \qquad (3.1)$$

Here $\bar{V}_i$ represents the partial molar volume of species i and the subscript V on (J_i) implies that each flux is measured with respect to the volume frame of reference.

The mathematical statement of Fick's first law for a binary system is

$$(J_i)_V = - (D_i)_V \, (\partial C_i / \partial z)_t \quad (i = 1,2), \tag{3.2}$$

where C_i is the concentration of component i expressed in moles per unit volume, the proportionality constant, $(D_i)_V$, is the diffusion coefficient and z specifies the direction of diffusion. By combining Equations (3.1) and (3.2) with the thermodynamic relation

$$\sum_{i=1}^{2} C_i \bar{V}_i = 1, \tag{3.3}$$

it is possible to show that

$$(D_1)_V = (D_2)_V = (\mathcal{D}_{12})_V , \tag{3.4}$$

where $(\mathcal{D}_{12})_V$ is the mutual diffusion coefficient.

3.3 The Cell Frame of Reference

Diffusion in *real* fluids is often complicated by volume changes which cause the system to experience a bulk flow. The volume-fixed reference frame cannot therefore be considered stationary[7] with respect to the cell frame. If u_{VC} denotes the relative velocity of the two frames and $(J_i)_C$ is the flux of component i in the cell frame, then the relationship between the two fluxes[4] is

$$(J_i)_C = (J_i)_V + C_i u_{VC} \quad (i = 1,2). \tag{3.5}$$

Kirkwood *et al.*[4] have shown that expressions for u_{VC} can be obtained from the equation

$$(\partial u_{VC}/\partial z)_t = - \sum_{i=1}^{2} \bar{V}_i \, [\partial (J_i)_V / \partial z]_t , \tag{3.6}$$

using the technique of integration by parts in conjunction with the particular boundary conditions defined by the diffusion cell geometry. For the immediate purpose these boundary conditions need only be specified as; at $z = 0$

$$(J_i)_v = (J_i)_c = 0 \quad (i = 1,2), \tag{3.7a}$$

and

$$u_{vc} = 0. \tag{3.7b}$$

These relationships correspond to the physical restriction of the cell being closed at $z = 0$.

Following further the procedure of Kirkwood *et al.*, Equation (3.5) can be expressed for component 1 as

$$(J_1)_c = - (\mathcal{D}_{12})_v \left(\frac{\partial C_1}{\partial z}\right) - C_1 \int_0^z \left(\frac{\partial \bar{V}_1}{\partial C_1}\right) \frac{(\mathcal{D}_{12})_v}{C_2 \bar{V}_2} \left(\frac{\partial C_1}{\partial x}\right)^2 dx. \tag{3.8}$$

Thus, if Fick's first law is to be applied in the cell frame of reference then the integral appearing in Equation (3.8) must vanish; the necessary condition being

$$(\partial \bar{V}_1 / \partial C_1) = 0 . \tag{3.9}$$

This condition is always applicable to *real gaseous systems* in the low density limit, whereas at greater densities restrictions on the nature of the systems chosen for study must be imposed if Equation (3.9) is to remain valid.

To determine the type of restriction, the *virial equation of state*[8] may be employed to evaluate the concentration dependence of the partial molar volumes (Appendix I). When this is done and third and higher virial coefficients are neglected, the result may be expressed as

$$(\partial \bar{V}_1 / \partial C_1) = - 4B_E C_2 / C^3 \bar{V}_2 \quad . \tag{3.10}$$

Here C is the *total* molar concentration and B_E is the excess second volume virial coefficient defined by

$$B_E = B_{12} - \tfrac{1}{2}(B_{11} + B_{22}) . \tag{3.11}$$

Comparison of Equations (3.9) and (3.10) implies that for moderate densities the restrictive condition is

$$B_E = 0. \tag{3.12}$$

In the situation where the partial molar volumes are *concentration dependent*, the integral in Equation (3.8) may still be neglected[4] by considering only small concentration gradients. However, for reasons discussed later, this procedure will not be adopted and it is necessary, therefore, to invoke the restriction specified by Equation (3.12) in order to obtain the relation

$$(J_i)_C = - (\mathcal{D}_{12})_V (\partial C_i / \partial z)_t \quad (i = 1,2). \tag{3.13}$$

Although direct application of Equation (3.13) is possible under steady state conditions[3], it is generally made use of in conjunction with the pertinent *equations of continuity*[5]. These latter relations describe the conservation of mass for each component and for those systems in which no chemical reactions occur, may be expressed as

$$[\partial (J_i)_C / \partial z]_t = - (\partial C_i / \partial t)_z \quad (i = 1,2). \tag{3.14}$$

Combining Equations (3.13) and (3.14) yields the partial differential equation

$$\left(\frac{\partial C_i}{\partial t}\right)_z = \left[\frac{\partial}{\partial z}\left(\mathcal{D}_{12}\frac{\partial C_i}{\partial z}\right)\right]_t \quad (i = 1,2), \tag{3.15}$$

where the subscript V has been omitted from $(\mathcal{D}_{12})_V$ for simplicity. This equation, commonly referred to as Fick's second law, takes the more convenient form

$$(\partial C_i/\partial t)_z = \mathcal{D}_{12}(\partial^2 C_i/\partial z^2)_t \quad (i = 1,2), \tag{3.16}$$

when the diffusion coefficient is independent of concentration.

In the special case where $\mathcal{D}_{12}$ is a *linear* function of concentration, Ljunggren[9] has shown that to a first approximation the diffusion coefficient may be considered constant with a value corresponding to that of the mean concentration of the experiment.

3.4 Restricted Diffusion

In order to obtain an expression for the concentration distribution, $C_i(z,t)$, from Equation (3.16) it is necessary to define certain experimental conditions. For this purpose, the diffusion vessel will be considered to take the form of a closed tube with a uniform cross section and a *finite* length, ℓ. If the upper and lower extremities of the cell are specified by the coordinates $z = 0$ and $z = \ell$ respectively, then the boundary conditions mentioned previously can be stated in full as

$$\partial C_i(0,t)/\partial z = \partial C_i(\ell,t)/\partial z = 0 . \tag{3.17}$$

The solution of Equation (3.16) subject to (3.17) is the Fourier series[10]

$$C_i(z,t) = \sum_{n=0}^{\infty} A_n \cos(n\pi z/\ell)\exp(-n^2\pi^2 \mathcal{D}_{12}\, t/\ell^2), \qquad (3.18)$$

where the coefficients, A_n, are related to the initial concentration distribution. This relationship permits the diffusion coefficient to be obtained from an analysis of the position and time dependence of the component concentrations.

3.5 The Classical Loschmidt Technique

Of the various experimental methods that have been developed to study gaseous diffusion, one of the first to be reported was due to Loschmidt[11] in 1870. The technique is based upon the formation of an initial *sharp* boundary between two gas mixtures enclosed within a cell similar to that outlined above. Defining the boundary position as $z = b$ and with reference to component 1, the initial experimental conditions may be stated as

$$C_1(z,0) = \begin{cases} C_1^u(0) & b < z < \ell \\ C_1^\ell(0) & 0 < z < b \end{cases} . \qquad (3.19)$$

Here $C_1^u(0)$ and $C_1^\ell(0)$ are the initial *uniform* concentrations in the upper and lower compartments.

The Fourier coefficients of Equation (3.18) can then be determined from[12]

$$A_0 = (1/\ell)\int_0^\ell C_1(z,t)\,dz, \qquad (3.20a)$$

$$A_n = (2/\ell)\int_0^\ell C_1(z,t)\cos(n\pi z/\ell)\,dz \quad (n \geqslant 1). \qquad (3.20b)$$

Evaluation of these integrals yields

$$A_0 = [b/\ell]C_1^{\ell}(0) + [(\ell-b)/\ell]C_1^{u}(0) = \bar{C}_1, \qquad (3.21a)$$

$$A_n = -\frac{2\Delta C_1}{n\pi}\sin(n\pi b/\ell) \quad (n \geqslant 1). \qquad (3.21b)$$

Here $\bar{C}_1$ is the concentration of component 1 averaged over the compartmental volumes and ΔC_1 is the initial concentration difference:

$$\Delta C_1 = C_1^{u}(0) - C_1^{\ell}(0). \qquad (3.22)$$

Substitution of Equations (3.21) in Equation (3.18) yields

$$C_1(z,t) = \bar{C}_1 - \frac{2\Delta C_1}{\pi}\sum_{n=1}^{\infty} a_n \exp(-n^2\pi^2 \mathcal{D}_{12}\, t/\ell^2), \qquad (3.23a)$$

with

$$a_n = \frac{1}{n}\sin\left(\frac{n\pi b}{\ell}\right)\cos\left(\frac{n\pi z}{\ell}\right) \quad (n \geqslant 1). \qquad (3.23b)$$

In a classical Loschmidt experiment the normal procedure is to isolate the two compartments about the position $z = b$ at some time , t , before complete mixing has occurred. Expressions for the average concentration in each compartment at this time can be obtained by integrating Equations (3.23) over the length of each compartment, *viz.*,

$$\langle C_1^{u} \rangle = \frac{1}{\ell-b}\int_b^{\ell} C_1(z,t)\,dz, \qquad (3.24a)$$

$$\langle C_1^{\ell} \rangle = \frac{1}{b}\int_0^{b} C_1(z,t)\,dz. \qquad (3.24b)$$

Hence,

$$\langle C_1^u \rangle = \bar{C}_1 + \frac{2\Delta C_1 \ell}{\pi^2(\ell-b)} \sum_{n=1}^{\infty} g_n \exp(-n^2\pi^2 \mathcal{D}_{12} t/\ell^2), \quad (3.25a)$$

$$\langle C_1^\ell \rangle = \bar{C}_1 - \frac{2\Delta C_1 \ell}{\pi^2 b} \sum_{n=1}^{\infty} g_n \exp(-n^2\pi^2 \mathcal{D}_{12} t/\ell^2), \quad (3.25b)$$

with

$$g_n = \frac{1}{n^2} \sin^2(n\pi b/\ell) \quad (n \geqslant 1). \quad (3.26)$$

These equations assume a much simpler form when $b = \ell/2$. In this case the quantity f, defined as

$$f = \frac{\langle C_1^u \rangle - \langle C_1^\ell \rangle}{\langle C_1^u \rangle + \langle C_1^\ell \rangle}, \quad (3.27)$$

can be related to $\mathcal{D}_{12}$ through

$$f = \frac{4\Delta C_1}{\pi^2 \bar{C}_1} \sum_{n=0}^{\infty} \frac{1}{(2n+1)^2} \exp[-(2n+1)^2\pi^2 \mathcal{D}_{12} t/\ell^2]. \quad (3.28)$$

If it is further assumed that initially each compartment contains a pure component, then Equations (3.21a) and (3.22) reduce to

$$\bar{C}_1 = \tfrac{1}{2} C_1^u(0), \quad (3.29a)$$

$$\Delta C_1 = C_1^u(0). \quad (3.29b)$$

Substituting into Equation (3.28) gives

$$f = \frac{8}{\pi^2} \sum_{n=0}^{\infty} \frac{1}{(2n+1)^2} \exp[-(2n+1)^2\pi^2 \mathcal{D}_{12} t/\ell^2]. \quad (3.30)$$

Thus, combination of the above expression with Equation (3.27) permits $\mathcal{D}_{12}$ to be calculated from the experimental quantities $\langle C_1^u \rangle$, $\langle C_1^\ell \rangle$, t and ℓ.

3.6 *The Continuous Analysis Method*

It is possible to utilise Equation (3.18) in a different manner to that described above by considering variations in concentration only at certain *positions* within the cell[3]. Dunlop and co-workers[13-16] have recently reported a similar technique whereby concentration *differences* are monitored as a function of time. Their method is similar to that developed by Harned[17] in order to study diffusion in electrolyte solutions.

The form of the equation on which the method is based can be derived simply from Equation (3.18) by evaluating $C_1(z,t)$ at $z = \ell/6$ and $5\ell/6$. Then by forming the difference

$$\Delta C_1(t) = C_1(\ell/6,t) - C_1(5\ell/6,t), \qquad (3.31)$$

it is possible to show

$$\Delta C_1(t) = A_1' \exp\left(-\frac{\pi^2 \mathcal{D}_{12} t}{\ell^2}\right) - A_5' \exp\left(-\frac{25\pi^2 \mathcal{D}_{12} t}{\ell^2}\right) + \ldots \quad . \qquad (3.32)$$

Here the coefficients A_n' are related to those of Equation (3.18) by

$$A_n' = \sqrt{3}\, A_n \quad (n \geqslant 1) \quad . \qquad (3.33)$$

For large values of time the second and higher order terms in Equation (3.32) become negligible. Thus by measuring the concentration difference or a property proportional to it, as a function of time, the diffusion coefficient can be determined.

A comparison of the experimental results obtained with the two techniques discussed above is given in Chapter VI.

REFERENCES

1. L. Dufour, *Pogg. Ann.* 148 490 (1873).

2. A. Fick, *Ann. Phys. Chem.* 94 59 (1955).

3. P.J. Dunlop, B.J. Steel and J.E. Lane in *Physical Methods of Chemistry*, Vol. I, edited by A. Weissberger and B. Rossiter, Wiley (1972).

4. J.G. Kirkwood, R.L. Baldwin, P.J. Dunlop, L.J. Gosting and G. Kegeles, *J. Chem. Phys.* 33 1505 (1960).

5. D.D. Fitts, *Non-equilibrium thermodynamics*, McGraw-Hill (1962).

6. G.S. Hartley and J. Crank, *Trans. Faraday Soc.* 45 801 (1949).

7. L. Onsager, *Ann. N.Y. Acad. Sci.* 46 241 (1945).

8. H. Kamerlingh Onnes, *Commun. Phys. Lab. Univ. Leiden*, No. 71 (1901).

9. S. Ljunggren, *Ark. Kemi.* 24 1 (1965).

10. J. Crank, *The Mathematics of Diffusion*, Oxford University Press (1957).

11. J. Loschmidt, *Akad. Wiss.Wien* 61 367 (1870).

12. R.D. Present, *Kinetic Theory of Gases*, McGraw-Hill (1958).

13. P.J. Carson, P.J. Dunlop and T.N. Bell, *J. Chem. Phys.* 56 531 (1972).

14. M.A. Yabsley and P.J. Dunlop, *J. Phys. E: Sci. Instrum.* 8 834 (1975).

15. G.R. Staker and P.J. Dunlop, *Rev. Sci. Instrum.* 47 1190 (1976).

16. K. Aoyagi, T.N. Bell and P.J. Dunlop, *J. Phys. E: Sci. Instrum.* 11 353 (1978).

17. H.S. Harned and D.M. French, *Ann. N.Y. Acad. Sci.* 46 267 (1945).

CHAPTER IV

EXPERIMENTAL APPARATUS AND PROCEDURE

4.1 Introduction

The solution of Fick's second law given in the previous chapter is based, in part, upon certain geometrical properties of the diffusion cell. In addition to these requirements, the cell must possess the ability to confine gases at elevated pressures. Special experimental procedures were also found to be necessary at these pressures. Particular reference is made to these aspects of cell design and experimental technique in the ensuing discussion. The manner in which Equations (3.27) and (3.30) are employed to calculate the diffusion coefficient will also be considered.

4.2 Cell Description

A diagram outlining the important features of the diffusion cell is shown in Figure 4.1. It is similar in design to cells previously employed in this[1,2] and other laboratories[3-6], and consists basically of two symmetrical sections or halves, joined together about a common pivot. Each half is comprised of a cylinder, closed at one end and attached to a disk in an off-centre position at the other. Both cylinders were constructed from a single stainless steel tube which had been honed out so that its internal diameter

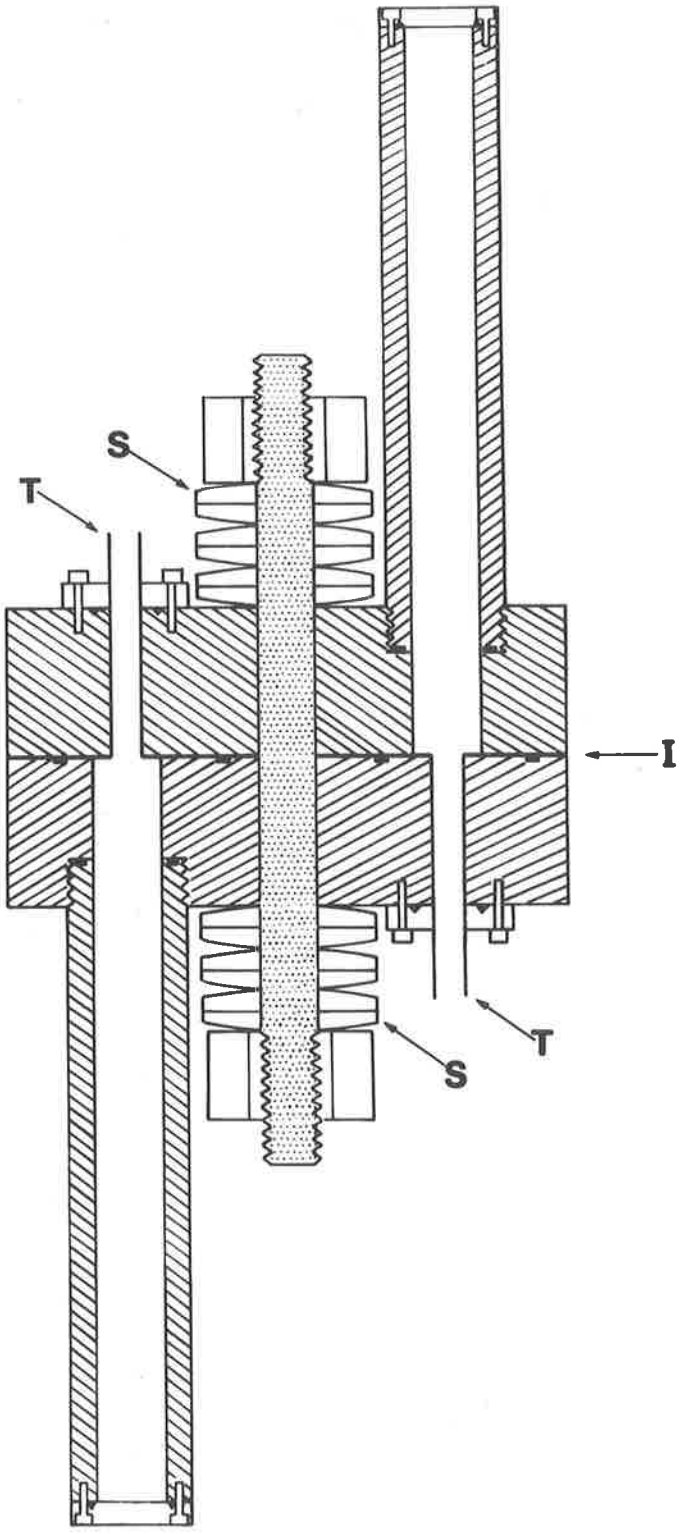

Figure 4.1: Loschmidt-type cell in section; S, springs, T, inlet and outlet vents, I, lapped surfaces, ■, viton O-ring, ▼, lead O-ring.

was constant to *better* than 0.001 cm. The discrepancy between the diameters of the cylinders and the connecting holes in the disks was also of this order of magnitude. Correspondingly, the variation in cross-sectional area over the length of the diffusion channel was less than 0.07%. The two disks, also manufactured from stainless steel, were 22.6 cm in diameter and 6.2 cm thick. They were clamped together by means of a spring system connected to a rod placed through their centres.

One problem associated with cells of this type is their susceptibility to leaks, particularly in the region of the interface between the cell halves. As a first precaution against such an occurrence, the mating surfaces of the disks were lapped against an optically flat stainless steel plate and against each other. A second safeguard consisted of two viton O-rings inserted between the disks into circular grooves concentric with the pivot. As the openings of the diffusion channel were contained within the annulus defined by the O-rings, external gas leaks were prevented. Before joining the disks together, a thin layer of Apiezon T-grease was applied to each surface to provide a vacuum seal and to aid lubrication. Finally, an intimate contact between the disks was ensured by employing a set of springs capable of exerting forces as great as 200 kN.

Other regions of the cell where a possibility of gas leakage exists are the ends of the diffusion channel and the connections between the cylinders and disks. The former sections were sealed with the aid of lead O-rings placed in

circular v-shaped grooves, while each of the latter was sealed by the insertion of a viton O-ring into an annular groove which had been cut in the end of the tube. Proper design of these grooves enabled the elimination of all free space between adjoining surfaces. To determine the success of these precautionary measures the cell was filled with nitrogen to a pressure of 20 atmospheres and isolated for 67 hours. Over this period of time the pressure was found to decrease by only 0.14%.

Since the magnitude of the relaxation time for a Loschmidt cell is dependent upon the cell length, as well as the diffusion coefficient, it was found necessary to manufacture three different pairs of cylinders. By interchanging these pairs, the cell length could be varied thus overcoming the problem of inordinately long diffusion periods. The lengths and internal diameters of these cells are summarised in Table 4.1.

Table 4.1

Dimensions of the Diffusion Cell

Cell designation	Length[a] (cm)	Internal diameter (cm)
C1	122.83	2.891
C2	60.00	2.890
C3	40.00	2.890

[a] The uncertainty in each length was believed to be less than 0.005 cm.

Great care was taken in the construction of each pair of cylinders to ensure that the cells were symmetrical about the interface. The actual position of this boundary as measured from the end of the lower compartment, and the ratio of the lower to upper compartmental volumes, R_v , are given in Table 4.2. A maximum error of 0.1% was estimated for the values of R_v and 0.005 cm for the boundary positions.

Table 4.2

Dimensions of the Cell Compartments

Cell designation	Boundary position (cm)	R_v
C1	61.41	1.000
C2	30.00	1.000
C3	20.00	1.000

The cell was suspended vertically in a water bath containing 500 litres of water; the lower half of the cell being held fixed in position. By rotating the upper section, with the assistance of a differential spur gear and pinion, the cell compartments could be aligned or separated. In this manner it was possible to form an initial boundary between the gases contained within the cell halves. When the compartments were fully separated, they were each positioned over a vent through which gases could be introduced or removed. The cell vents were connected to the external apparatus, comprising gas cylinders, vacuum system and pressure gauges, by a manifold constructed from stainless steel tubing.

4.3 *Experimental Procedure*

All experiments were performed by filling each evacuated cell compartment with a pure gas and then aligning the cell when thermal equilibrium had been attained. Diffusion was allowed to proceed for a measured period of time, t, before separating the compartments. During the filling procedure, the problem of an *internal* gas leak, via the interface, became significant whenever a large pressure gradient existed between the cell halves. This problem was solved by *alternately* adding gas to each compartment so that the pressure difference became progressively less as the final pressure was approached. The last additions of gas were monitored very carefully to make certain that the final compartmental pressures were the same. Gravitational stability was maintained during diffusion by always filling the lower compartment with the more dense gas.

Pressure measurements were made using a series of Texas Instruments Bourdon-tube gauges. Two of the Bourdon-tubes consisted of quartz spirals and were intended for use over pressure ranges of 0 to 1 and 0 to 14 atmospheres. Another tube, of aluminium, was employed for measurements between 13 and 30 atmospheres. The two high pressure gauges were calibrated against a dead weight tester (Bell and Howell, type 6-201-0001 primary pressure standard) in this laboratory. These calibrations were reproducible to within 0.03% and were corrected to account for the difference between the local gravitational acceleration[7] ($9.79724\ ms^{-2}$) and the standard value ($9.80665\ ms^{-2}$); the accuracy of the dead weight tester was stated as being better than 0.025%. The low pressure tube

was calibrated against a similar pressure standard at the Ion Diffusion Unit, Research School of Physical Sciences, Australian National University.

The period of time during which diffusion occurred was chosen to be in the region of an *optimum* time[8], t_{opt}, defined by

$$t_{opt} = \ell^2/\pi^2 \mathcal{D}_{12} \quad . \tag{4.1}$$

This diffusion time minimises the effect of certain experimental errors on the derived value of $\mathcal{D}_{12}$ and is discussed in more detail in Chapter VI. Optimum times for all experiments were greater than 7000 seconds. As the alignment and separation of the compartments required a finite interval of time, this diffusion period was uncertain to the extent of ±6 seconds.

After the optimum period of time had elapsed, the compartments were rotated into a position where they were separated from each other but were not in communication with the vents. The cell was left in this configuration until the compartmental concentrations became uniform. A period of approximately $3t_{opt}$ was necessary for this mixing to occur (see Appendix II). The vents, which still contained the original component gases, were then evacuated before rotating the compartments further. During evacuation, any internal leak *between* each compartment and vent was unimportant because the two mixtures were uniform in concentration.

Throughout all experiments, the temperature of the thermostat bath was controlled to within ±0.005K with an on-off mercury-toluene relay[9]. Mercury-in-glass thermometers,

which had been calibrated against a platinum resistance thermometer, were used to monitor the bath temperature.

4.4 *Calculation of the Diffusion Coefficient*

Slightly different forms of Equations (3.27) and (3.30) were used to calculate $\mathcal{D}_{12}$.

Equation (3.30) was simplified by neglecting the second and higher order terms which amount to no more than 0.004% of the first term when $t \geqslant t_{opt}$. Thus

$$f = \frac{8}{\pi^2} \exp(-\pi^2 \mathcal{D}_{12}\, t/\ell^2) . \qquad (4.2)$$

Final compartmental concentrations were analysed in terms of the component molefractions, x_i . These could be converted to the concentrations, C_i , appearing in Equation (3.27), by utilising the virial equation of state. The necessary relationship being

$$C_i = x_i\ P/Z_m RT \quad (i = 1,2) . \qquad (4.3)$$

Here P, T and R denote the pressure, absolute temperature and gas constant, respectively, and Z_m is the virial expansion:

$$Z_m = 1 + B'_m\ P + \ldots . \qquad (4.4)$$

B'_m is the second pressure virial coefficient which is defined for a binary mixture as

$$B'_m = \sum_{i=1}^{2} \sum_{j=1}^{2} x_i\, x_j\ B'_{ij} . \qquad (4.5)$$

Substitution of Equation (4.3) in (3.27) yields, after several manipulations,

$$f = [\langle x_1^u \rangle Z_\ell - \langle x_1^\ell \rangle Z_u] / [\langle x_1^u \rangle Z_\ell + \langle x_1^\ell \rangle Z_u], \qquad (4.6)$$

where $\langle x_1^u \rangle$ and $\langle x_1^\ell \rangle$ are the final upper and lower molefractions, respectively; Z_u and Z_ℓ are the corresponding values of Z_m.

The combination of Equations (4.2) and (4.6) enables $\mathcal{D}_{12}$ to be determined from $\langle x_1^u \rangle$, $\langle x_1^\ell \rangle$, t, P, ℓ and the virial coefficient data. In order that these two equations be consistent, the component 1 referred to in the latter equation always denotes the *lighter* of the two components.

4.5 *Mass Balance Relationship*

In the absence of any leaks the total mass of each component must remain constant throughout all experiments. Thus it is possible to compare the amount of each component present initially, with the amount present at the end of the experiment. A convenient way of performing this comparison is to consider the mean molefraction, $\bar{x}_1$, which can be calculated from the initial conditions and also from the final analysed concentrations.

When the initial conditions are considered, $\bar{x}_1$ can be expressed as

$$\bar{x}_1 = V_u C_1^u(0) / (V_u C_1^u(0) + V_\ell C_2^\ell(0)). \qquad (4.7)$$

Here V_u and V_ℓ denote the upper and lower compartment volumes. Simplifying this expression with the aid of Equation (4.3), one obtains

$$\bar{x}_1 = Z_2 / (Z_2 + R_V Z_1), \qquad (4.8)$$

where

$$Z_i = 1 + B'_{ii} P + \ldots \quad (i = 1,2), \tag{4.9a}$$

and

$$R_V = V_\ell / V_u \quad . \tag{4.9b}$$

For the second type of calculation, the mean mole-fraction is represented as $\bar{x}_1(\text{exp})$ and is derived in a similar fashion to Equation (4.8). The resulting expression is

$$\bar{x}_1(\text{exp}) = \frac{\langle x_1^u \rangle Z_\ell + \langle x_1^\ell \rangle Z_u R_V}{Z_\ell + Z_u R_V} \quad . \tag{4.10}$$

While agreement between $\bar{x}_1$ and $\bar{x}_1(\text{exp})$ does not in itself signify a successful experiment, disagreement does imply an unsuccessful experiment. When comparing these values a discrepancy arising from the expected maximum experimental errors in $\langle x_1^u \rangle$ and $\langle x_1^\ell \rangle$ must be allowed for. The magnitudes of such errors are discussed in Chapter V.

For the purpose of summarising the comparison of $\bar{x}_1(\text{exp})$ and $\bar{x}_1$ over a range of pressures, Equation (4.8) was expanded as a Taylor series in P:

$$\bar{x}_1 = (1+R_V)^{-1} + \frac{R_V (B'_{22} - B'_{11})}{(1+R_V)^2} P + \ldots \quad . \tag{4.11}$$

When R_V is close to unity the above expression can be simplified, without introducing any significant error, by substituting ¼ for $R_V/(1+R_V)^2$. That is

$$\bar{x}_1 = (1+R_V)^{-1} + \tfrac{1}{4}(B'_{22} - B'_{11})P + \ldots \quad . \tag{4.12}$$

Another consequence of such values of R_v is that to a good approximation, Equation (4.10) may be written as

$$\bar{x}_1(\text{exp}) = \frac{\langle x_1^u \rangle Z_\ell + \langle x_1^\ell \rangle Z_u}{Z_\ell + Z_u} \quad . \tag{4.13}$$

If the values of $\bar{x}_1(\text{exp})$ are then fitted to an equation of the form

$$\bar{x}_1(\text{exp}) = a_0 + a_1 P \ , \tag{4.14}$$

the derived constants, a_0 and a_1, can be compared with the predicted values $(1+R_v)^{-1}$ and $\frac{1}{4}(B'_{22} - B'_{11})$.

REFERENCES

1. G.R. Staker, M.A. Yabsley, J.M. Symons and P.J. Dunlop, *J.C.S. Faraday Trans.I* 70 825 (1974).

2. G.R. Staker and P.J. Dunlop, *Chem.Phys. Letters* 42 419 (1976).

3. L.E. Boardman and N.E. Wild, *Proc. Roy. Soc. (London)* A162 511 (1937).

4. F.T. Wall and G.A. Kidder, *J. Phys. Chem.* 50 235 (1946).

5. R.A. Strehlow, *J. Chem.Phys.* 21 2101 (1953).

6. J.N. Holsen and M.R. Strunk, *Ind. Eng. Chem. Fundam.* 3 143 (1964).

7. J. McG. Hall, *Report of the Gravitational Stations in the Metropolitan Area and Salisbury*, South Australian Dept. of Mines, Report 59/89 (1964).

8. D.P. Shoemaker and C.W. Garland, *Experiments in Physical Chemistry*, McGraw-Hill (1974).

9. R.H. Stokes, *New Zealand J. Sci. Technol. B* 27 75 (1945).

CHAPTER V

CONCENTRATION ANALYSIS

5.1 Introduction

Determination of the diffusion coefficient, using the method described in Chapter IV, depends ultimately upon being able to measure the final compartmental concentrations. For this purpose a mass spectrometric technique was adopted, in preference to a method employed previously in this laboratory[1,2] which exploited the difference between the thermal conductivities of the component gases. This choice made it possible to study those systems in which the component masses differed but the thermal conductivity difference was negligible. In particular, it was anticipated that the mass spectrometer would eventually be employed in studies of isotopic systems.

The experimental method briefly referred to at the end of Chapter III has been implemented by using thermistors to monitor the thermal conductivity difference[1], and thus the concentration difference between the cell positions $\ell/6$ and $5\ell/6$. Although this method and the classical Loschmidt technique cannot be classified as being truly independent, the use of the mass spectrometer in the latter helps minimise the similarities between them. Comparison of the results obtained with both procedures is them somewhat more meaningful.

5.2 The Mass Spectrometer

All analyses were performed with a Micromass MM6 mass spectrometer which is based upon a 6 cm, 90° deflection sector. Ions were formed by bombardment with electrons from a thoriated-iridium filament; the electron energies were fixed at 70 ev. The mass spectrum was scanned by varying the current through the deflecting electromagnet. Fixed ion-accelerating voltages of 700 and 350 volts were employed for the mass ranges 2-50 and 2-100 amu respectively.

Because the spectrometer was used primarily for quantitative measurements on mixtures whose component masses differed significantly, the sensitivity of the instrument was of more importance than its resolution. The resolving section therefore consisted of a set of slits, 0.1 cm in width, which optimised the sensitivity at the expense of resolution. As a further consequence the component peaks were flat-topped, thus facilitating the measurement of their heights.

The mass spectrometer vacuum system consisted of a polyphenyl ether oil diffusion pump and a two-stage rotary pump. A cold trap was employed, but only to act as a baffle. A butterfly valve, through which had been drilled a small hole, was inserted between the diffusion pump and cold trap. During each analysis this valve was closed and the system pumped through the hole. The resulting decrease in pumping speed caused an approximate ten-fold increase in pressure and an associated increase in ion current magnitude. This arrangement also acted as a choke which decreased the

effect of any pumping speed variations. After an analysis was completed the valve was opened in order to effectively pump out the spectrometer. Pressures of 10^{-7} torr were attainable with the valve open and 10^{-6} - 10^{-5} torr with it closed.

Ion currents were detected with a single Faraday plate collector connected to a VG-Micromass CA2 chopper amplifier. The input stage of the latter consisted of a 10^{11} ohm resistor and varactor diode bridge amplifier which possessed a stability similar to that of a vibrating reed amplifier[3]. Output from the chopper amplifier was fed to a 3490A Hewlett-Packard digital voltmeter interfaced to a 9810A HP programmable calculator. In this way an arbitrary number of peak height measurements, each requiring 0.270 seconds, could be summed and the average obtained.

5.3 Sample Introduction System

Any mass spectrometric analysis of the relative abundance of components within a mixture is complicated by the problem of relating the component proportions in the ionization region to those in the parent sample[4,5]. In the case of gaseous mixtures, this problem arises because of the nature of the gas flow from the sample reservoir,through a constriction of some type, to the ionization chamber. If the sample pressure is so low that the mean free path of the molecules is large when compared with the constriction dimensions, then the flow of gas through the constriction is termed *molecular flow*[6]. Here the flow of each component is

inversely proportional to the square root of its mass and hence *mass discrimination* or *fractionation* occurs in this region. This type of sample introduction system is known as a *molecular leak*. Since the flow through the spectrometer is also molecular, the ratio of the component partial pressures in the ionization chamber is the same as that in the sample container when a steady state flow has been attained. However, the major disadvantage of the molecular leak is the fractionation at the constriction which causes the relative concentrations in a finite sample reservoir to change with time. Consequently a different type of inlet system, the *viscous leak*, was adopted.

The viscous leak differs from the molecular leak in two aspects. Firstly, a long thin capillary tube is placed between the sample reservoir and constriction and,secondly, the use of larger sample pressures permits *viscous flow* through the capillary. Although fractionation still occurs at the constriction, where viscous flow blends into molecular flow, its effect on the sample concentration can be minimised by a certain choice[7] of capillary and reservoir dimensions.

Kistemaker[7], and Halsted and Nier[8] have derived equations which approximate the flow of a binary gas mixture through a viscous leak. The important results of their work can be summarised as:-

(i) Long narrow capillaries and small constrictions produce the largest fractionation, however, capillaries of such dimensions also reduce the effect of back diffusion on the sample concentration.

(ii) Before any measurements can be made a certain period of time must be allowed for the attainment of steady state flow.

(iii) It is important to ensure that sample pressures are identical when comparing different analyses.

(iv) The sample reservoir should preferably have a volume greater than 100 cm^3.

Because the corresponding mathematical results cannot generally be used in an *a priori* fashion to calculate the actual behaviour of such a leak, a process of calibration with mixtures of known composition was employed.

The viscous leak supplied by the spectrometer manufacturer consisted of a stainless steel capillary 90 cm in length, 0.015 cm in diameter, with a crimping device attached to the spectrometer end. A sample reservoir of approximately 1200 cm^3 in volume was connected to the other end of the capillary. The flow rate against atmospheric pressure was nominally set at 0.02 cm^3/min, giving an analyser pressure of 10^{-4} torr when pumped at 2 litre/sec. Sample pressures were in the region 150 - 200 torr and were monitored by means of a Schlumberger transducer or a Texas Instruments pressure gauge. During the time required to analyse a gas mixture the sample pressure changed by less than 0.3%.

5.4 Concentration Determination

Calibration of the mass spectrometer with standard mixtures is further necessitated when the relationship between the component ion current and concentration in the ion source

is considered. One must *assume* that for a given sample concentration, the ion current ratio is proportional to the ratio of concentrations in the sample gas[9], that is

$$I_2/I_1 \propto \beta(x_2/x_1). \qquad (5.1)$$

Here x_i denote the sample gas molefractions and I_i the ion currents. β depends upon factors[9] such as the characteristics of the leak system, the difference in ionization probabilities of the components, the difference between the collection yields of the ion beams and any nonlinearity possibly inherent in the amplifying system. As the peak heights are measured in terms of an amplified voltage, h_i, which is proportional to I_i, Equation (5.1) may be employed in the form

$$x_2/x_1 = S_r(h_2/h_1), \qquad (5.2)$$

where S_r is termed an "apparent sensitivity ratio" and is similar to the mass spectrometer bias referred to by Walton and Cameron[10]. Accordingly, S_r is treated as a characteristic of the mass spectrometer and inlet system and must be determined by calibration.

All analyses involved the measurement of the peak heights of both gases until their *ratio* remained constant to *better* than 0.1% for at least three pairs of averages. Each average consisted of 500 individual measurements requiring approximately 135 seconds to complete. The period of time necessary for the peak height ratio to attain this measure of constancy depended upon the nature of the system. For the

binary combinations of N_2, O_2 and Ar it was in the region 90 - 110 minutes and for the system Ar + Kr it was approximately 140 minutes.

Individual peak heights were corrected for the presence of small background peaks measured prior to admitting a gas sample. A *memory effect*[9] was noticeable for those systems which contained either O_2 or Kr. In these cases the background attained a constant magnitude only after allowing a gas sample to flow through the spectrometer for at least 30 minutes. Thus the practice of priming the mass spectrometer with a mixture containing those components that were to be analysed was adopted.

Analyses of unknown mixtures and calibrations were performed in identical fashions. After measurements were completed on one mixture the spectrometer and sample reservoir were pumped out and the background measured again, before the introduction of the next mixture. Peak heights for all systems studied varied between 1 and 4 volts depending on the relative concentrations. The zero of the amplifier was adjusted to give an average value of less than 10^{-4} volts and was checked between each pair of peak height measurements.

Before Equation (5.2) can be used in order to calculate x_1 from measurements of (h_2/h_1), it is necessary to determine how S_r depends on concentration. Such an investigation, whereby a series of mixtures with known compositions were analysed, was performed for the N_2 + Ar system. The results of these experiments are summarised in Table 5.1 and Figure 5.1. It was observed that over the concentration range

Table 5.1[a]

Mass Spectrometer Calibrations for N_2 + Ar

Calibration A		Calibration B		Calibration C	
x_2	S_r	x_2	S_r	x_2	S_r
0.3814	0.5864	0.3814	0.5855	0.4357	0.5863
	0.5866		0.5857	0.6222	0.5886
	0.5865		0.5857	0.7752	0.5907
0.4357	0.5874	0.5874	0.5893		0.5911
	0.5878	0.7752	0.5933		
0.5874	0.5910				
	0.5908				
	0.5907				
0.6222	0.5907				
0.7752	0.5947				
	0.5946				
intercept	0.5787	intercept	0.5782	intercept	0.5803
slope	0.0204	slope	0.0192	slope	0.0136
ave.dev.	±0.05%	ave.dev.	±0.03%	ave.dev.	±0.04%

[a] In each case S_r was fitted to a linear function of x_2. The intercept at $x_2 = 0$, the slope and the average deviation of the experimental points from each straight line are also listed in the table.

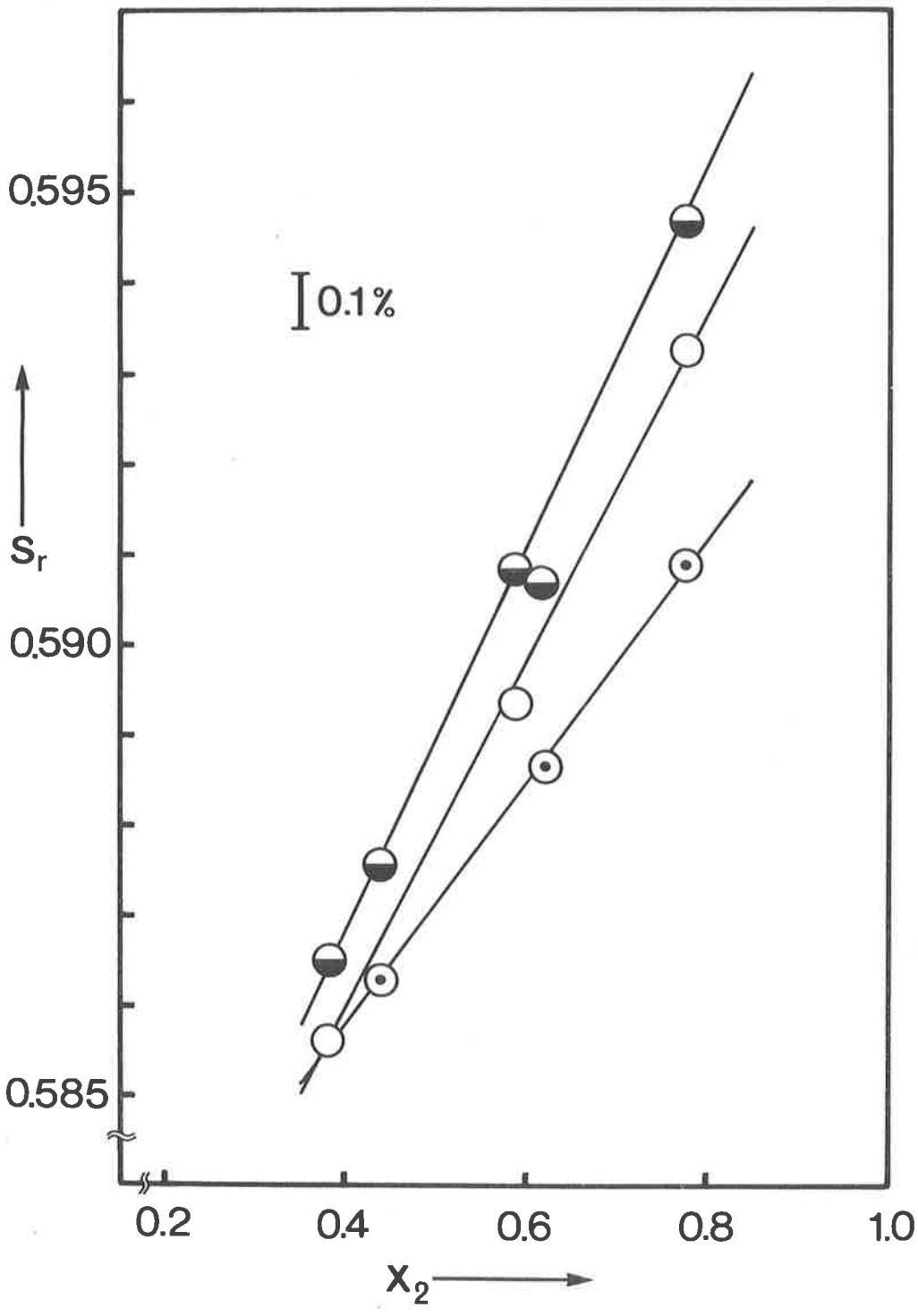

Figure 5.1: Apparent sensitivity ratios, S_r, versus x_2 for the N_2 + Ar system; ◒, calibration A, ○, calibration B, ⊙, calibration C. Duplicate and triplicate points are not indicated in the figure.

studied, S_r could be adequately described by a *linear* function of molefraction; a result similar to that reported by Walton and Cameron[10] for the $^{20}Ne + {}^{22}Ne$ system. Thus when calibrating the mass spectrometer, at least two mixtures with different compositions should be used.

Inspection of Figure 5.1 also shows that the three calibrations illustrated differ by an amount greater than the experimental precision. Such variations from day to day are typical[11] of an electron impact ionization source.

For systems other than $N_2 + Ar$, the linear dependence of S_r was *assumed*. This is not an unreasonable approximation if at least one of the calibration mixtures has a molefraction in the neighbourhood of that which is to be measured. Furthermore, since two mixtures must be analysed in order to obtain a value of $\mathcal{D}_{12}$, it is logical to perform one calibration at a molefraction close to $\langle x_1^u \rangle$ and the other at a molefraction close to $\langle x_1^\ell \rangle$. Once the two values of S_r have been determined, the constants a and b appearing in

$$S_r = a x_1 + b, \tag{5.3}$$

can be evaluated. Then, by employing this equation in conjunction with Equation (5.2), values of $\langle x_1^u \rangle$ and $\langle x_1^\ell \rangle$ can be calculated from the corresponding peak height ratio measurements. In these calculations it is more convenient to use a rearranged form of Equation (5.2):

$$x_1 = [1 + S_r (h_2/h_1)]^{-1}, \tag{5.4}$$

and adopt an iterative method of solution.

5.5 *Calibration Mixtures*

To remove the need for accurate measurements of volume, pressure and virial coefficient data, calibration mixtures were prepared *by weight*. A balance (Voland Corp. U.S.A., model HCE 10 equal arm mass comparator) capable of weighing a mass of 10 kg with a sensitivity of ±0.001g was employed for this purpose.

Gas mixtures were prepared in Matheson size 6 cylinders which had previously been evacuated and baked out. The external surfaces of these cylinders were chrome-plated to prevent oxidation.

All weighings were performed against a tare and the appropriate buoyancy corrections made. The final concentration of any mixture, although calculated from the actual masses of the gases, could be crudely controlled by monitoring the pressure from the source cylinders. For the majority of mixtures at least 20g of each component were weighed; the maximum error in such weights being less than 0.005g. The effect of these errors on the value of x_1 can be estimated from

$$\left|\frac{dx_1}{x_1}\right| \leq x_2\left|\frac{dm_1}{m_1}\right| + x_2\left|\frac{dm_2}{m_2}\right| \quad , \tag{5.5}$$

where m_1 and m_2 denote the masses of the two components. If mixtures are prepared so as to have molefractions near 0.65 and 0.35, then

$$\left|\frac{dx_1}{x_1}\right|_{x_1=0.65} < 2 \times 10^{-4} \quad , \tag{5.6a}$$

and

$$\left|\frac{dx_1}{x_1}\right|_{x_1=0.35} < 3 \times 10^{-4} \quad . \tag{5.6b}$$

These values of molefraction correspond approximately to $\langle x_1^u \rangle$ and $\langle x_1^\ell \rangle$.

5.6 *Errors in Concentration Determination*

Consider the case where a molefraction, x_1, has to be measured. Two calibrations are performed, one at a molefraction, x_1^c, in the region of x_1.

An estimation of the experimental error in x_1 can be made by differentiating Equation (5.4). This yields

$$\left|\frac{dx_1}{x_1}\right| \leq x_2 \left|\frac{dS_r}{S_r}\right| + x_2 \left|\frac{d(h_2/h_1)}{(h_2/h_1)}\right| . \qquad (5.7)$$

Similarly, it is possible to derive from Equations(5.2) and (5.5) the expression

$$\left|\frac{dS_r^c}{S_r^c}\right| \leq \left|\frac{d(h_2/h_1)_c}{(h_2/h_1)_c}\right| + \left|\frac{dm_1}{m_1}\right| + \left|\frac{dm_2}{m_2}\right| , \qquad (5.8)$$

where S_r^c and $(h_2/h_1)_c$ pertain to x_1^c. The peak height ratios were accurate to approximately 0.1% while the uncertainties in m_1 and m_2 have been discussed above. Substitution of these values into Equation (5.8) gives

$$\left|\frac{dS_r^c}{S_r^c}\right| < 0.0015. \qquad (5.9)$$

This error can be related to that in S_r by expressing Equation (5.3) as

$$S_r = S_r^c + a(x_1 - x_1^c). \qquad (5.10)$$

If x_1^c is chosen so that $|x_1 - x_1^c| < 0.05$, then

$$\left|\frac{dS_r}{S_r}\right| < 0.002, \qquad (5.11)$$

and thus

$$\left|\frac{dx_1}{x_1}\right| < 0.003\ x_2 \quad . \qquad (5.12)$$

Applying this final relationship to the quantities $\langle x_1^u \rangle$ and $\langle x_1^\ell \rangle$ gives

$$\left|\frac{d\langle x_1^u \rangle}{\langle x_1^u \rangle}\right| < 0.001 \ , \qquad (5.13a)$$

$$\left|\frac{d\langle x_1^\ell \rangle}{\langle x_1^\ell \rangle}\right| < 0.002 \ . \qquad (5.13b)$$

These predictions can be tested by using the data given in Table 5.1. If two of the points from each set of calibrations are used to define S_r, then the others can be treated as mixtures of unknown composition and their molefractions calculated. The average discrepancy between the molefractions determined by weighing and those determined by mass spectrometric analysis is 0.07%.

As further evidence, a Loschmidt experiment was simulated by preparing four N_2 + Ar mixtures; two of which would be used for calibration purposes while the other pair would be substituted for the cell compartment mixtures. These results, summarised in Tables 5.2 and 5.3, vindicate Equations (5.13a) and (5.13b).

Table 5.2[d]

Loschmidt Experiment Simulation: Calibration

x_1	S_r	a	b
0.3046	0.5927		
0.7120	0.5901	-6.38×10^{-3}	0.5946

[d] The quantities a and b refer to those of Equation (5.3).

Table 5.3[a]

Loschmidt Experiment Simulation: Analysis

	(h_2/h_1)	x_1 (measured)	x_1 (actual)
"upper compartment"	0.8565	0.6641	0.6643
"lower compartment"	3.356	0.3346	0.3349

[a] x_1 (actual) is the value of molefraction determined by weighing while x_1 (measured) is that calculated from the mass spectrometric analysis.

Finally, inspection of the raw experimental data tabulated in the appendices reveals that when experiments are analysed in *duplicate*, the discrepancies between the measured molefractions are *less than* the values specified by Equations (5.13).

REFERENCES

1. M. A. Yabsley and P.J. Dunlop, *J. Phys. E: Sci. Instrum.* 8 834 (1975).

2. J.M. Symons, M.L. Martin and P.J. Dunlop, J.C.S. *Faraday Trans. I* (in press).

3. Technical data, VG-Micromass Ltd., Winsford, Cheshire, England.

4. H.A. Tasman, A.J.H. Boerboom and J. Kistemaker, in *Mass Spectrometry* edited by C.A. McDowell McGraw-Hill (1963).

5. M.G. Inghram, *Advan. Electron. Electron Phys.* 1 232 (1948).

6. M. Knudsen, *Ann. Physik (IV)* 28 75 (1909).

7. J. Kistemaker, *Physica* 18 163 (1952).

8. R.E. Halsted and A.O. Nier, *Rev. Sci. Instrum.* 21 1019 (1950).

9. W.G. Mook and P.M. Grootes, *Int. J. Mass Spectrom. Ion. Phys.* 12 273 (1973).

10. J.R. Walton and A.E. Cameron, *Z. Naturforsch.* 21a 115 (1966).

11. R.A. Saunders, *J. Phys. E: Sci. Instrum.* 1 1053 (1968).

CHAPTER VI

EXPERIMENTAL ACCURACY

6.1 Introduction

The effect of any uncertainty in the experimental quantities used in calculating the diffusion coefficient can be estimated quite readily by differentiating Equation (4.2). That is

$$\left|\frac{d\mathcal{D}_{12}}{\mathcal{D}_{12}}\right| \leqslant 2\left|\frac{d\ell}{\ell}\right| + \left|\frac{dt}{t}\right| + \frac{\ell^2}{\pi^2\mathcal{D}_{12}t}\left|\frac{df}{f}\right| \quad . \tag{6.1}$$

Other types of errors caused by factors such as the Dufour effect, heat-of-mixing and a concentration dependent diffusion coefficient are more difficult to determine; these will be considered in a more general fashion. A comparison of the experimental techniques employed in this laboratory is given at the end of the chapter.

6.2 Errors in f

It will be shown that the major contribution to error in $\mathcal{D}_{12}$ arises from that in f; however, this error can be reduced by selecting the diffusion period which minimises[1] $(\partial\mathcal{D}_{12}/\partial f)$. This value of time is the optimum value referred to in Chapter IV. When $t \geqslant t_{opt}$, the relationship (6.1) simplifies to

$$\left|\frac{d\mathcal{D}_{12}}{\mathcal{D}_{12}}\right| \leq 2\left|\frac{d\ell}{\ell}\right| + \left|\frac{dt}{t}\right| + \left|\frac{df}{f}\right| \quad . \tag{6.2}$$

Another type of optimum diffusion period has been discussed by Tordai[2] but it is applicable only when the approximation

$$f = 1 - 4(\mathcal{D}_{12}\, t/\ell^2\pi)^{\frac{1}{2}} \quad , \tag{6.3}$$

is valid. That is, for small values of t. It is also evident that the relative error in f is decreased by the use of the maximum *initial* concentration difference in each Loschmidt experiment.

The uncertainty in f is primarily dependent upon errors in $\langle x_1^u \rangle$ and $\langle x_1^\ell \rangle$ and to a certain extent upon errors in the virial coefficient data. Neglection of third and higher order virial coefficients introduced no significant uncertainty. The second virial coefficient data used[3] were believed accurate to within $\pm 2\times10^{-5}$ atm^{-1} while the mole-fraction errors have been estimated (§5.6). Consequently, an error propagation analysis of Equation (4.6) yields for the maximum cumulative error in f :

$$\left|\frac{df}{f}\right| < 0.005; \quad P \leq 25 \text{ atm.} \tag{6.4}$$

6.3 Cell Dimensions

The accuracy with which the cell dimensions could be measured is given in §4.2. Although the cell length is the only cell dimension that enters directly into the equations employed to calculate $\mathcal{D}_{12}$, these equations are based upon the assumptions of uniform cross-sectional area and symmetry about the interface.

The uncertainty in the total length of the cell can be related to that in $\mathcal{D}_{12}$ through the first term of Equation (6.2); for the largest of the cells used this error is insignificant, while for the smallest it can amount to an error of 0.025% in the diffusion coefficient.

To determine the effect of a discrepancy, δ, between the boundary position and $z = \ell/2$, it is convenient to write Equations (3.25) in the form

$$\langle C_1^u \rangle = \bar{C}_1(\delta) + \frac{2\ell}{\ell - 2\delta} \sum(\delta), \tag{6.5a}$$

$$\langle C_1^\ell \rangle = \bar{C}_1(\delta) - \frac{2\ell}{\ell + 2\delta} \sum(\delta) . \tag{6.5b}$$

Here

$$\sum(\delta) = \frac{2\Delta C_1}{\pi^2} \sum_{n=1}^{\infty} \frac{1}{n^2} \sin^2\left(\frac{n\pi}{2} + \frac{n\pi\delta}{\ell}\right) \exp(-n^2\pi^2 \mathcal{D}_{12}\, t/\ell^2), \tag{6.6a}$$

and

$$\bar{C}_1(\delta) = \tfrac{1}{2}[C_1^u(0) + C_1^\ell(0)] - \Delta C_1\, \delta/\ell . \tag{6.6b}$$

Hence the correct expression for f is

$$f = \left[\frac{4\ell^2 \Sigma(\delta)}{\ell^2 - 4\delta^2}\right]\left[2\bar{C}_1(\delta) + \frac{8\ell\delta\Sigma(\delta)}{\ell^2 - 4\delta^2}\right]^{-1} . \tag{6.7}$$

Expanding f as a Taylor series in δ gives

$$f = f_0 + 2f_0(1 - f_0)(\delta/\ell) + \ldots , \tag{6.8a}$$

where

$$f_0 = \frac{8}{\pi^2} \exp(-\pi^2 \mathcal{D}_{12}\, t/\ell^2) \; ; \quad t \geqslant t_{opt} . \tag{6.8b}$$

Thus the relative error produced in assuming cell symmetry, that is, equating f and f_0, is approximately $2(1 - f_0)\delta/\ell$.

Since $|\delta| \leq 0.005$ cm, this contributes no more than 0.02% to the uncertainty in $\mathcal{D}_{12}$.

The extent of the inaccuracy introduced by a non-uniform cross-sectional area is difficult to ascertain. However, if reasonable care is taken with the construction of the cell this error should be minimal.

6.4 *Alignment and Isolation of the Cell Compartments: Error in t*

As a consequence of the method of cell alignment and isolation, certain experimental conditions lack the complete definition necessary for the solution of the diffusion equation. Such complications can be summarised as:-

(i) What particular stages during the opening and closing mark the limits of the diffusion period?

(ii) Uncertainty in the form of the initial boundary in that it is not a perfectly sharp horizontal boundary. A similar uncertainty is introduced when the compartments are separated.

(iii) The actual physical movement of one compartment with respect to the other may cause turbulent mixing.

Bunde[4] has considered problem (i) for a Loschmidt cell with rectangular cross-section. He has shown that the correct zero time can be taken as that instant when the compartments are half aligned. This result is contingent upon the assumptions of constant alignment velocity and constant mass flux during the period of alignment. For a cell of circular cross-section and by similar reasoning, the zero time corresponds

to approximately 42% alignment. Since the isolation of the compartments can be treated in an analogous fashion and is in fact a *complementary* situation, timing may be commenced at any point during alignment as long as it is concluded at the same point during isolation.

The undefined nature of the initial boundary is a result of the horizontal concentration gradients formed during compartment alignment. Because this perturbation decays with time[5], the concentration distribution must approach that described by Equations (3.23). However, the exact zero time of this distribution is uncertain. Similarly, any initial turbulence, which results in a transport of mass additional to the normal diffusion process, can be treated as causing inaccuracy in t.[2,4] Again, analogous arguments may be employed for the separation of the compartments. As the neglection of such effects should have greater bearing on experiments of short duration, indirect evidence concerning the significance of any consequent error can be obtained by comparing the results of experiments with different diffusion times. For this comparison it is important to ensure that the magnitudes of any other experimental errors remain constant in relation to the different values of t. Hence, optimum diffusion periods were still used but were varied by altering the cell length. Inspection of the results summarised in Table 6.1 reveals no evident trend in PD_{12} with respect to variations in t. Therefore the supposition that this type of error is relatively insignificant seems reasonable.

Table 6.1

Effect of Duration on Observed Diffusion Coefficient

System	ℓ (cm)	P (atm)	t (s)	$P\mathcal{D}_{12}$ (atm $cm^2 s^{-1}$)
N_2 + Ar	122.83	4.001	29520	0.2032
	60.00	4.001	7140	0.2031
	122.83	6.001	45000	0.2031
	60.00	6.004	11160	0.2029
N_2 + O_2	60.00	15.975	26880	0.2160
	40.00	15.977	12000	0.2162

Boyd *et al.*[6] have also studied the behaviour of the initial boundary using a cell made of Lucite and an optical schlieren apparatus. No evidence of turbulence was discovered but the boundary was found to possess a degree of obliqueness which was dependent upon the alignment velocity. This latter effect, however, soon disappeared once the compartments were completely aligned.

For the purpose of making a crude estimation of such errors in t, the intervals of time required to open and close the cell were treated as the sole source of uncertainty, that is

$$\left|\frac{dt}{t}\right| \leqslant 0.001 \ . \qquad (6.9)$$

6.5 *Concentration Dependent Diffusion Coefficient*

When the diffusion coefficient does depend upon concentration, the correct form of Fick's second law is

$$(\partial C_i/\partial t) = \mathcal{D}_{12}(\partial^2 C_i/\partial z^2) + (\partial \mathcal{D}_{12}/\partial C_i)(\partial C_i/\partial z)^2 . \qquad (6.10)$$

As yet, no analytical solution of this equation for the case of a Loschmidt cell has been proposed. This inevitably leads to the use of approximations which reduce the magnitude of the second term of Equation (6.10) with respect to the first.

The measured composition dependences of $\mathcal{D}_{12}$ at one atmosphere and 300K, for all but one of the systems studied, are given in Table 6.2. These results were best represented by a linear function of molefraction, *viz.*,

$$\mathcal{D}_{12} = \mathcal{D}^0_{12}(1 + ax_2) \ . \qquad (6.11)$$

Data for the N_2 + Ar system were taken from reference 7, Ar + Kr from reference 8, while the O_2 + Ar data were obtained using a two-bulb apparatus[9] and experimental method described elsewhere.[10]

Table 6.2

Composition Dependence of $\mathcal{D}_{12}$ at 300K

System	$\mathcal{D}^0_{12}$ ($cm^2 s^{-1}$)	$a \times 10^3$	Av. Dev.[b] (%)
N_2 + Ar	0.2034	4.1	±0.04
Ar + Kr	0.1404	2.6	±0.05
O_2 + Ar	0.2037	2.5	±0.02

[b] These figures represent the average percentage deviation of the experimental points from the least-square line.

It can be seen that for these three systems the maximum variation of $\mathcal{D}_{12}$ with concentration is about 0.4%. For the other system of interest, N_2 + O_2, theoretical calculations[11] predict that the composition dependence is even less. Given the small extent of this dependence and noting the result of Ljunggren mentioned in §3.3, it is reasonable to assume the simplest form of Fick's second law.

6.6 *Pressure and Temperature*

The temperature of the thermostat bath could be measured to within ±0.002K; temperature variations during the diffusion period were never greater than ±0.005K. On this basis alone, any resultant inaccuracy in $\mathcal{D}_{12}$ is negligible.

Another point of interest in relation to temperature variations is the effect of convection within the cell. However, in this instance, the temperature control was considered good enough to preclude significant convection.

Pressure measurements were accurate to approximately 0.06%. Consequently, an error of similar magnitude is introduced into the quantity $P\mathcal{D}_{12}$ in addition to the other errors inherent in the diffusion coefficient. For the product $n\mathcal{D}_{12}$, the number density, n, can be calculated from P using

$$n = P/z_m kT \ , \qquad (6.12)$$

and is uncertain to the extent of about 0.1%. The *precision* with which pressures could be reproduced is also of importance in ensuring a negligible difference between the initial compartmental pressures. Calibration of the pressure gauges indicated that the reproducibility of the gauge reading was better than 0.03%.

Although the pressure and temperature could be determined within well defined limits, various non-ideality and kinetic phenomena may cause deviations from isothermal and isobaric conditions. The temperature of a diffusing gas

mixture is disturbed by both the heat-of-mixing and the Dufour effect. The former is due to the real nature of the gas system and its magnitude, at moderate densities, can be approximated by[12]

$$\tilde{H}^E = 2x_1 x_2 P[B_E - T(dB_E/dT)] \quad . \qquad (6.13)$$

Here $\tilde{H}^E$ is the excess molar enthalpy of mixing and B_E has been defined previously (Equation (3.11)). Even though the heat-of-mixing increases with pressure and is maximised when pure gases mix, estimations based on the above equation show that $\tilde{H}^E$ is extremely small for the systems $N_2 + O_2$, $N_2 + Ar$, $O_2 + Ar$ and $Ar + Kr$. The Dufour effect refers to the transient temperature difference produced by a concentration gradient and can be regarded as the inverse of thermal diffusion. In general, the magnitude of the temperature difference is small when the component masses are comparable[13,14] and can be further reduced by a suitable choice of cell dimensions.[5] That is, if the cross-sectional area of the cell is small, the temperature gradients are rapidly dissipated by conduction to the cell walls. As a function of pressure, Mason *et al.*[15] have observed that the maximum temperature difference increases with P whereas the rate at which it decays decreases. Thus any inaccuracy caused by the Dufour effect should be more pronounced at higher pressures.

The mixing of real gases within a vessel of fixed volume can also result in pressure changes. Obviously this must create uncertainty in the value of $\mathcal{D}_{12}$ which varies approximately with the inverse of P. Another consequence is the invalidation of Fick's first law in the cell frame of reference. The size

of the pressure change, ΔP_{mix} , is again a function of B_E (see Appendix I); example calculations of ΔP_{mix} for the mixing of two pure components in a Loschmidt-type cell are given in Table 6.3. These data indicate that ΔP_{mix} is generally of the order of the error in P .

Table 6.3[a]

Pressure-of-mixing at 300K and $x_1 = 0.5$

System	P_{max} (atm)	$\Delta P_{mix}/P_{max}$ (%)
N_2 + Ar	25	-0.03
N_2 + O_2	25	0.01
O_2 + Ar	25	0.07
Ar + Kr	10	0.09

[a] P_{max} refers to the maximum pressure at which diffusion experiments were performed.

A further pressure gradient may arise during diffusion because of a difference in the average molecular velocities[16] . However such gradients are negligible except for the case of diffusion within a capillary.

6.7 Comparison with other Experimental Results

The other experimental method extensively employed for gaseous diffusion studies in this laboratory, namely the continuous analysis or thermistor bridge method, has been well

documented elsewhere[17]. Briefly, it consists of monitoring the difference in resistance, $\Delta R(t)$, of the two thermistors until *complete* mixing has occurred. Assuming ΔR is proportional to ΔC_1, then

$$\Delta R(t) = A' \exp(-\pi^2 \mathcal{D}_{12} t/\ell^2) + \Delta R(\infty), \qquad (6.14)$$

where $\Delta R(\infty)$ is the difference in resistance at equilibrium (*c.f.* Equation (3.32)). If $\Delta R(t)$ is measured at *regular intervals* of time, then $\mathcal{D}_{12}$ can be determined via a curve fitting procedure. Diffusion coefficients at pressures of one atmosphere or less have been measured for a large number of binary gas systems with this method; an experimental precision of sometimes better than 0.1% but never worse than 0.2% has been obtained[18].

An initial comparison of the two techniques using the N_2 + Ar system and a Loschmidt cell specifically designed for the thermistor method[19] is summarised in Table 6.4. The thermistors were left in the cell during the classical type experiments; lower pressures were used in the thermistor experiments so as to permit convenient relaxation times. Agreement between the two sets of data is excellent.

Classical Loschmidt experiments performed in the cell manufactured for this study also yielded a value of 0.2037 atm $cm^2 s^{-1}$ for $P\mathcal{D}_{12}$. Other comparative data for different systems and temperatures are listed in Table 6.5.

While the thermistor bridge method is only a variation upon the Loschmidt technique, there are some important differences between it and the classical method. Most significantly, the thermistor method is relatively insensitive to

Table 6.4[a]

Comparison of Classical Loschmidt and Thermistor Bridge Techniques for N_2 + Ar at 300K and x_1 = 0.5

Classical Loschmidt		Thermistor Bridge	
P (atm)	PD_{12} (atm $cm^2 s^{-1}$)	P (atm)	PD_{12} (atm $cm^2 s^{-1}$)
0.9459	0.2036	0.2139	0.2036
0.9675	0.2036	0.4255	0.2036
0.9549	0.2039	0.2361	0.2039
0.9560	0.2036	0.5002	0.2038
0.9904	0.2040	0.5002	0.2037
0.9468	0.2037		
0.9510	0.2035		

[a] The cell used was 117.34 cm in length.

Table 6.5[a]

Further Comparison between Classical and Thermistor Bridge Methods

System	T (K)	Classical Loschmidt PD_{12} (atm $cm^2 s^{-1}$)	Thermistor Bridge PD_{12} (atm $cm^2 s^{-1}$)
N_2 + Ar	323.16	0.2323	0.2325 (20)
O_2 + Ar	300.00	0.2037	0.2039
Ar + Kr	300.00	0.1406	0.1405 (8)
	323.16	0.1612	0.1615 (8)

[a] All diffusion coefficients were measured at x_1 = 0.5 and near 1 atm; where thermistor results are taken from literature reference is given in brackets.

the form of the initial conditions. This is because measurements of $\Delta R(t)$ are not commenced until some time after alignment of the cell compartments. Therefore any initial perturbations that may exist have time to decay and the coefficient A', in equation (6.14), will be ultimately independent of t. Although in this situation A' is unknown, only its constancy is mandatory for thermistor experiments. Evidence for this hypothesis was obtained by performing N_2 + Ar thermistor bridge experiments in which an initial pressure difference was purposefully created. Values of $P\mathcal{D}_{12}$ were calculated using the average or final pressure, $\bar{P}$, defined by

$$\bar{P} = \tfrac{1}{2}(P_u + P_\ell). \qquad (6.15)$$

Inspection of Table 6.6 reveals no noticeable discrepancy between these data and the results of equal-pressure experiments. Thus the concordance between the thermistor and classical methods lends support to the assumptions concerning the initial conditions of the latter technique.

Furthermore, as the thermistors themselves are extremely sensitive to temperature changes, the Dufour effect and heat-of-mixing are more likely to cause inaccuracy in the thermistor bridge method. However, no such disturbances were detectable at pressures near one atmosphere and hence the agreement between this method and the classical Loschmidt technique is even more encouraging.

Table 6.6

N_2 + Ar Thermistor Experiments with Initial Pressure Difference ΔP

x_1	$\bar{P}$ (atm)	$\Delta P/\bar{P}$ (%)	$\bar{P}\mathcal{D}_{12}$ (atm $cm^2 s^{-1}$)	$P\mathcal{D}_{12}$[a] (atm $cm^2 s^{-1}$)
0.476	0.2100	-10	0.2037	0.2038
0.524	0.2100	10	0.2037	0.2038
0.550	0.2000	20	0.2037	0.2038
0.575	0.2000	30	0.2035	0.2037

[a] Results of equal-pressure experiments taken from data of Table 6.2.

It was not possible to compare the two experimental procedures at higher pressures because the thermistor method fails for systems other than those containing excess helium[17]. The exact reasons for this failure have not been determined but may lie in the increased magnitudes of the Dufour and heat-of-mixing effects, or be due to an increase in free convection from the thermistors[21].

For the purpose of comparison with the results of other workers, the correlation function of Marrero and Mason[22] has been used to predict values of $P\mathcal{D}_{12}$ for the relevant systems. These predictions along with the present experimental results are given in Table 6.7.

Table 6.7

Comparison with Other Results

System ($T=300K, x_1=0.5$)	Predicted value[a] $P\mathcal{D}_{12}$ (atm $cm^2 s^{-1}$)	Classical Loschmidt $P\mathcal{D}_{12}$ (atm $cm^2 s^{-1}$)	Δ (%)
N_2 + Ar	0.198 (3%)	0.2037	+2.9
N_2 + O_2	0.211 (3%)	0.2192	+3.9
O_2 + Ar	0.195 (3%)	0.2037	+4.5
Ar + Kr	0.140 (1%)	0.1406	+0.4

[a] Figures in brackets represent the quoted uncertainties.

The small discrepancy between the diffusion coefficients for Ar + Kr is particularly pleasing in that the experimental determinations upon which the correlation function is based are much more accurate[22] in this case.

In summary, the accumulation of those errors that have been numerically estimated in the foregoing discussion gives rise to a possible maximum uncertainty of ±0.7% in $P\mathcal{D}_{12}$. This compares favourably with the average experimental precision of ±0.2%.

REFERENCES

1. D.P. Shoemaker and C.W. Garland, *Experiments in Physical Chemistry*, McGraw-Hill (1974).

2. L. Tordai, *Brit. J. App. Phys.* 1 329 (1950).

3. J.H. Dymond and E.B. Smith, *The virial coefficients of gases*, Clarendon Press (1969).

4. R.E. Bunde, *Univ. Wisconsin Naval Research Lab.* Report No. CM-850 (1955).

5. S. Ljunggren, *Ark. Kemi.* 24 1 (1965).

6. C.A. Boyd, N. Stein, V. Steingrimsson and W.F. Rumpel, *J. Chem Phys.* 19 548 (1951).

7. P.S. Arora, I.R. Shankland, T.N. Bell, M.A. Yabsley and P.J. Dunlop, *Rev. Sci. Instrum.* 48 673 (1977).

8. P.S. Arora, P.J. Carson and P.J. Dunlop, *Chem. Phys. Letters* 54 117 (1978).

9. P.S. Arora, H.L. Robjohns and P.J. Dunlop, *Physica* (in press).

10. M.A. Yabsley and P.J. Dunlop, *Physica* 85A 160 (1976).

11. J.O. Hirschfelder, C.F. Curtiss and R.B. Bird, *Molecular Theory of Gases and Liquids*, (4th printing) Wiley (1967).

12. M. Knoester, K.W. Taconis and J.J.M. Beenakker, *Physica* 33 389 (1967).

13. K. Clusius and L. Waldmann, *Die Naturwiss.* 30 711 (1942).

14. L. Miller, *Z. Naturforsch.* 4a 262 (1949).

15. E.A. Mason, L. Miller and T.H. Spurling, *J. Chem. Phys.* 47 1669 (1967).

16. K.P. McCarty and E.A. Mason, *Phys. Fluids* 3 908 (1960).

17. G.R. Staker and P.J. Dunlop, *Chem. Phys. Letters* 42 419 (1976), and references cited therein.

18. P.J. Dunlop, private communication.

19. G.R. Staker, M.A. Yabsley, J.M. Symons and P.J. Dunlop, *J.C.S. Faraday Trans. I* 70 825 (1974).

20. P.S. Arora, H.L. Robjohns, I.R. Shankland and P.J. Dunlop, *Chem. Phys. Letters* 59 479 (1978).

21. G.R. Staker, P.J. Dunlop, K.R. Harris and T.N. Bell, *Chem. Phys. Letters* 32 561 (1975).

22. T.R. Marrero and E.A. Mason, *J. Phys. Chem. Ref. Data* 1 3 (1972).

CHAPTER VII

EXPERIMENTAL DENSITY DEPENDENCE

7.1 Introduction

All numerical results derived from individual classical Loschmidt experiments are tabulated in Appendix III (Tables III.3 - 9); the second virial coefficients required for calculations of $\mathcal{D}_{12}$, n and $\bar{x}_1$(exp) are listed in Tables III.1 and III.2.

Before entering into a discussion of the density dependence of the diffusion coefficient the variation of $\bar{x}_1$(exp) with P is examined in the context of Equations (4.12) and (4.14). In the latter sections of the chapter, the experimental dependence of $n\mathcal{D}_{12}$ on n is compared with both the Enskog-Thorne result for rigid spheres and an empirical modification of the theory.

7.2 Pressure Dependence of $\bar{x}_1$(exp)

As stated in §4.5, comparison of $\bar{x}_1$ and $\bar{x}_1$(exp) serves as a negative indication of the success of an experiment. Given the possible maximum errors in $\langle x_1^u \rangle$, $\langle x_1^\ell \rangle$, B'_{ij} and R_V, then $\bar{x}_1$(exp) should be accurate to within ±0.16%. Values of the average discrepancy, Δ_{ave}, and the average absolute discrepancy, $|\Delta|_{ave}$, between $\bar{x}_1$ and $\bar{x}_1$(exp) are given in Table 7.1. These data all lie *within* the expected

error in $\bar{x}_1$(exp); the negative Δ_{ave} values could possibly be attributed to a small consistent error in the determinations of $\langle x_1^u \rangle$ and $\langle x_1^\ell \rangle$ or R_V being slightly greater than unity.

Table 7.1[a]

Average Discrepancies between $\bar{x}_1$ *and* $\bar{x}_1$*(exp)*

System	T (K)	Δ_{ave} (%)	$\lvert\Delta\rvert_{ave}$ (%)
N_2 + Ar	300.00	-0.07	0.07
	323.16	-0.06	0.06
N_2 + O_2	300.00	-0.12	0.11
	323.16	-0.08	0.08
O_2 + Ar	300.00	-0.02	0.03
Ar + Kr	300.00	-0.03	0.06
	323.16	-0.04	0.06

[a] $\Delta = \bar{x}_1(\text{exp}) - \bar{x}_1$.

For each system and temperature the $\bar{x}_1$(exp) data were fitted to an equation similar in form to (4.14), *viz.*,

$$\bar{x}_1(\text{exp}) = a_0 + a_1 P \ , \tag{7.1}$$

and the comparisons

$$a_0 \equiv (1 + R_V)^{-1} \ , \tag{7.2a}$$

$$a_1 \equiv \tfrac{1}{4}(B'_{22} - B'_{11}) \ , \tag{7.2b}$$

made on the basis of arguments outlined in §4.5. Least-squares

Table 7.2: $\bar{x}_1$ (exp) versus P , Data for Equation (7.1)

System	T (K)	a_0	10^4 Error[b]	$10^4 a_1$ (atm^{-1})	10^4 Error[b] (atm^{-1})	10^4 Std.Dev.[c]
N_2 + Ar	300.00	0.4996	± 1.3	- 1.14	± 0.10	2.6
	323.16	0.4998	± 3.1	- 1.09	± 0.24	2.6
N_2 + O_2	300.00	0.4996	± 1.3	- 1.27	± 0.09	2.2
	323.16	0.4995	± 2.7	- 0.97	± 0.21	2.2
O_2 + Ar	300.00	0.4998	± 0.8	0.09	± 0.08	1.1
Ar + Kr	300.00	0.5001	± 3.7	- 4.26	± 0.73	2.9
	323.16	0.4996	± 3.6	- 2.42	± 0.67	2.5

[b] Errors in a_0 and a_1 quoted to 95% confidence limits.

[c] Standard deviation of $\bar{x}_1$ (exp) values.

parameters for Equation (7.1) are listed in Table 7.2 and the variation of $\bar{x}_1$(exp) with P illustrated in Figures 7.1 and 7.2.

Table 7.3 contains a series of R_V values calculated from Equation (7.2a); these are in good agreement with the value 1.000 ± 0.001 determined from measurements of the cell dimensions.

Table 7.3

Values of R_V Calculated from a_0

System	T (K)	R_V
N_2 + Ar	300.00	1.0016±0.0005
	323.16	1.0008±0.0012
N_2 + O_2	300.00	1.0016±0.0005
	323.16	1.0020±0.0011
O_2 + Ar	300.00	1.0008±0.0003
Ar + Kr	300.00	0.9996±0.0015
	323.16	1.0016±0.0014

Comparison of a_1 with $\frac{1}{4}(B'_{22} - B'_{11})$ is summarised in Table 7.4. In order to determine the likely uncertainty in $\frac{1}{4}(B'_{22} - B'_{11})$, errors in the B'_{ii} data were taken from the literature.[1] Inspection of this table shows that the two quantities agree within the limits of their mutual uncertainties.

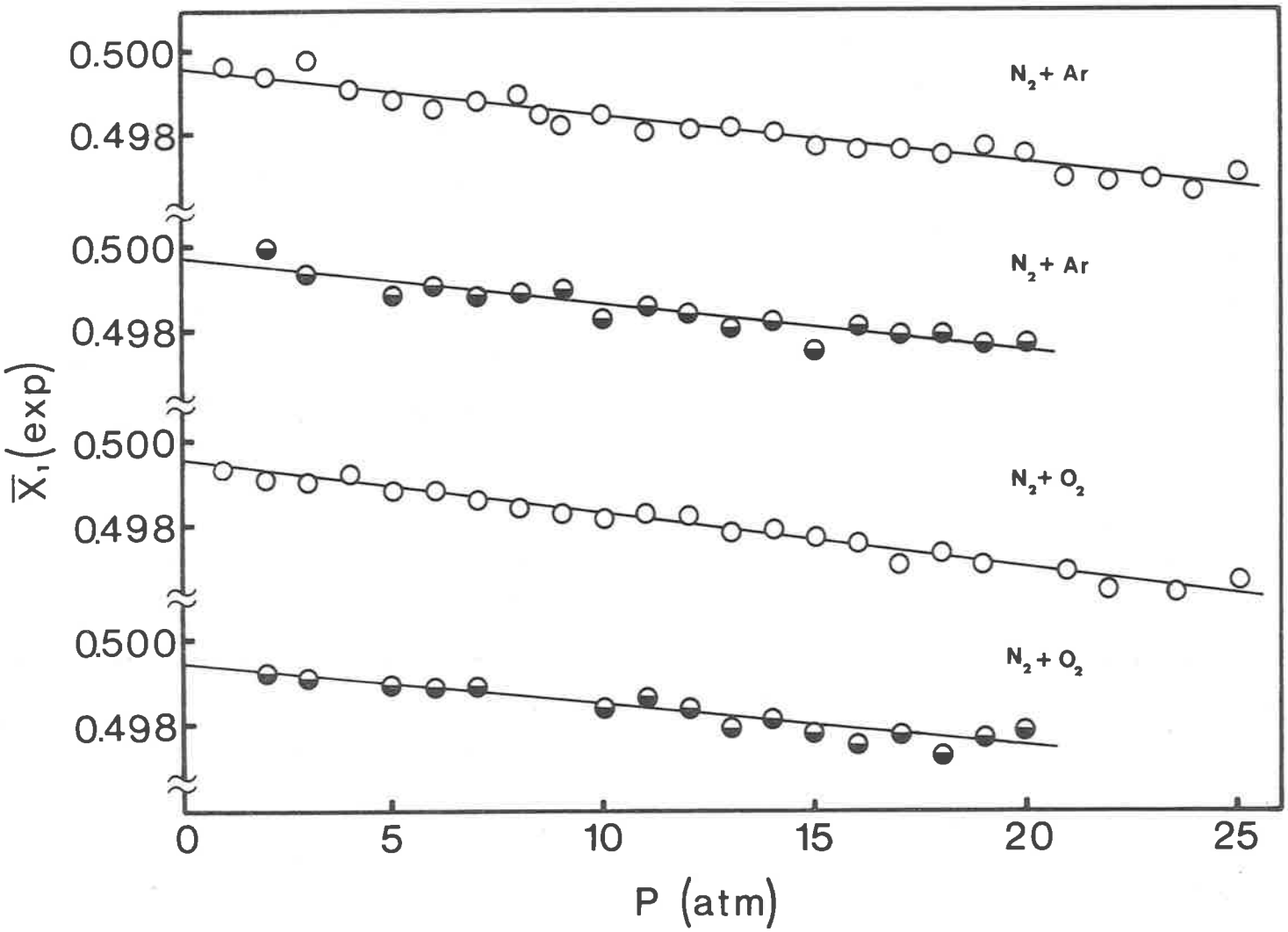

Figure 7.1: Pressure dependence of $\bar{x}_1(exp)$ for the N_2 + Ar and N_2 + O_2 systems; ○, 300.00K, ◒, 323.16K. Multiplicate points are not indicated in the Figure.

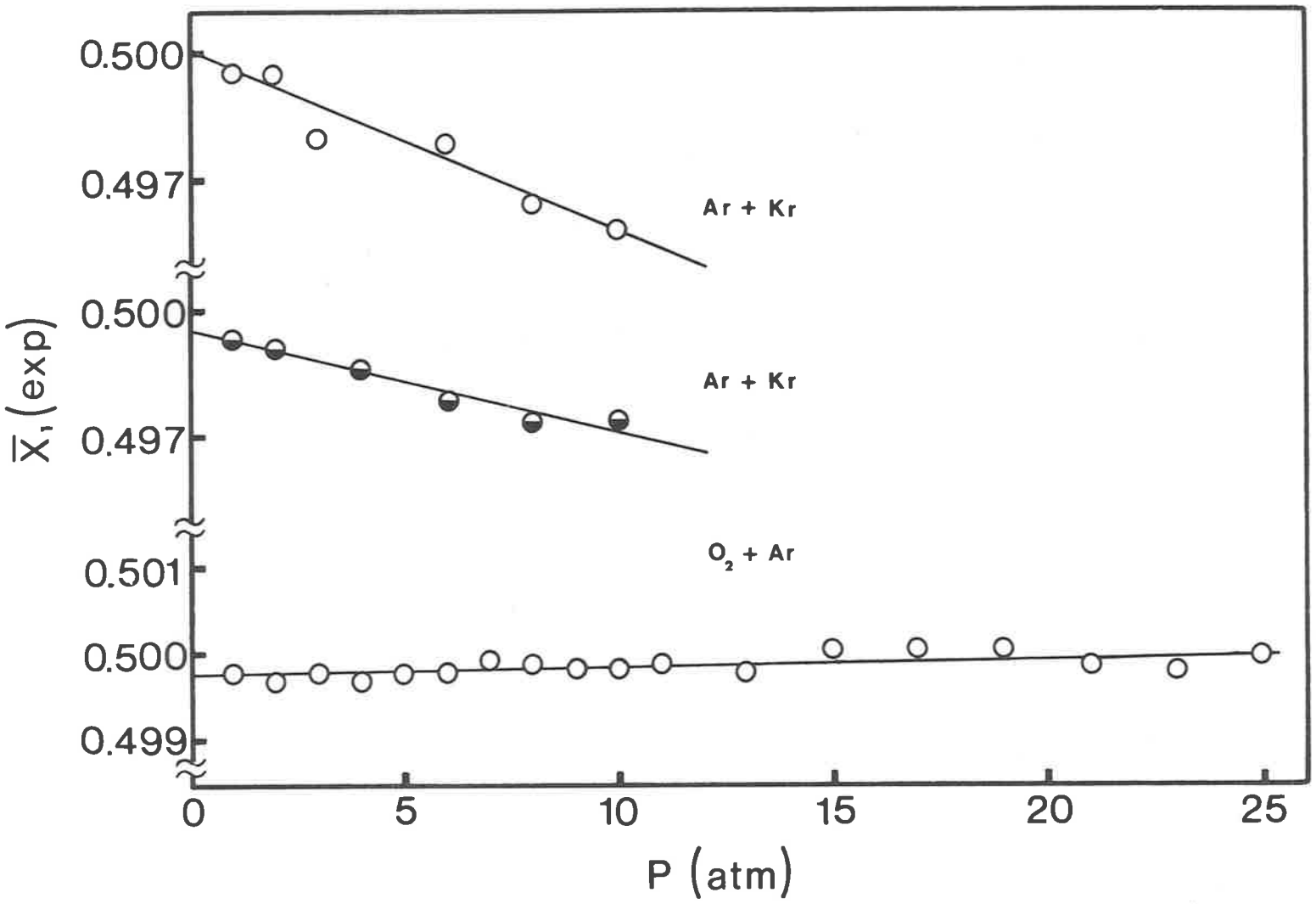

Figure 7.2: Pressure dependence of $\bar{x}_1$(exp) for the Ar + Kr and O_2 + Ar systems; ○, 300.00K, ◒, 323.16K. Multiplicate points are not indicated in the Figure.

Table 7.4

Comparison of a_1 with $\frac{1}{4}(B'_{22} - B'_{11})$

System	T (K)	$10^4\ a_1$ (atm^{-1})	$10^4[\frac{1}{4}(B'_{22} - B'_{11})]$ (atm^{-1})
N_2 + Ar	300.00	-1.14±0.1	-1.16±0.1
	323.16	-1.09±0.2	-1.03±0.1
N_2 + O_2	300.00	-1.27±0.1	-1.15±0.2
	323.16	-0.97±0.2	-1.06±0.2
O_2 + Ar	300.00	0.09±0.1	-0.04±0.2
Ar + Kr	300.00	-4.26±0.7	-3.54±0.2
	323.16	-2.42±0.7	-2.90±0.2

7.3 Density Dependence Results

Experimental diffusion data are summarised here in terms of the equations

$$P\mathcal{D}_{12} = (P\mathcal{D}_{12})_0 (1 + \theta P), \qquad (7.3)$$

and

$$n\mathcal{D}_{12} = (n\mathcal{D}_{12})_0 (1 + B_D n) . \qquad (7.4)$$

These relationships were found to reproduce the data within the experimental precision. The coefficients $(P\mathcal{D}_{12})_0$, θ, $(n\mathcal{D}_{12})_0$ and B_D along with their respective errors are given in Tables 7.5 and 7.6. All errors quoted apply to a 95% confidence limit. Figures 7.3 - 6 illustrate graphically the dependence of $n\mathcal{D}_{12}$ on n.

Table 7.5: Least-square Parameters for Equation (7.3)

System	T (K)	$(P\mathcal{D}_{12})_0$ (atm $cm^2 s^{-1}$)	10^4 Error (atm $cm^2 s^{-1}$)	10^4 θ (atm^{-1})	10^4 Error (atm^{-1})	10^4 Std. Dev. (atm $cm^2 s^{-1}$)
N_2 + Ar	300.00	0.2038	± 1.0	- 9.16	± 0.4	1.9
	323.16	0.2325	± 3.3	- 6.84	± 1.2	2.9
N_2 + O_2	300.00	0.2194	± 1.1	- 9.43	± 0.4	1.8
	323.16	0.2501	± 3.6	- 6.48	± 1.1	2.9
O_2 + Ar	300.00	0.2038	± 1.9	-10.1	± 0.9	2.6
Ar + Kr	300.00	0.1409	± 2.3	-21.9	± 3.2	1.8
	323.16	0.1614	± 2.8	-20.6	± 3.3	2.0

Table 7.6: Least-square Parameters for Equation (7.4)

System	T (K)	$10^{-20}(n\mathcal{D}_{12})_0$ ($m^{-1}s^{-1}$)	10^{-23} Error ($m^{-1}s^{-1}$)	10^{29} B_D (m^3)	10^{29} Error (m^3)	10^{-23} Std. Dev. ($m^{-1}s^{-1}$)
N_2 + Ar	300.00	4.987	± 2.4	- 2.08	± 0.1	4.7
	323.16	5.279	± 7.6	- 2.00	± 0.2	6.5
N_2 + O_2	300.00	5.368	± 2.7	- 2.22	± 0.2	4.7
	323.16	5.680	± 7.5	- 1.85	± 0.2	6.4
O_2 + Ar	300.00	4.987	± 4.5	- 1.53	± 0.3	6.3
Ar + Kr	300.00	3.447	± 5.7	- 3.31	± 1.3	4.6
	323.16	3.666	± 6.1	- 4.54	± 1.4	4.2

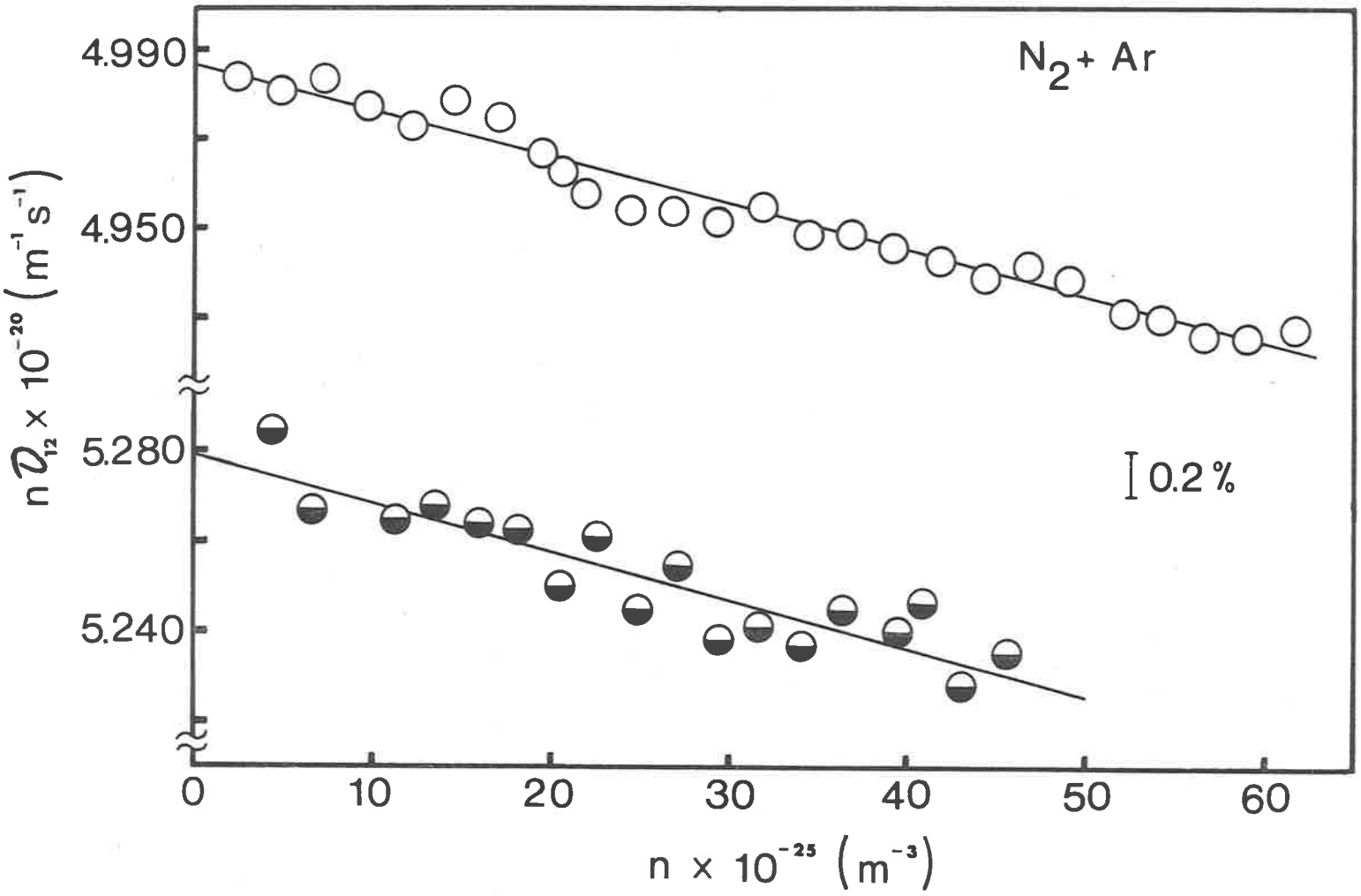

Figure 7.3: Density dependence of $n\mathcal{D}_{12}$ for the N_2 + Ar system; ○, 300.00K, ◒, 323.16K. Multiplicate points are not indicated in the Figure.

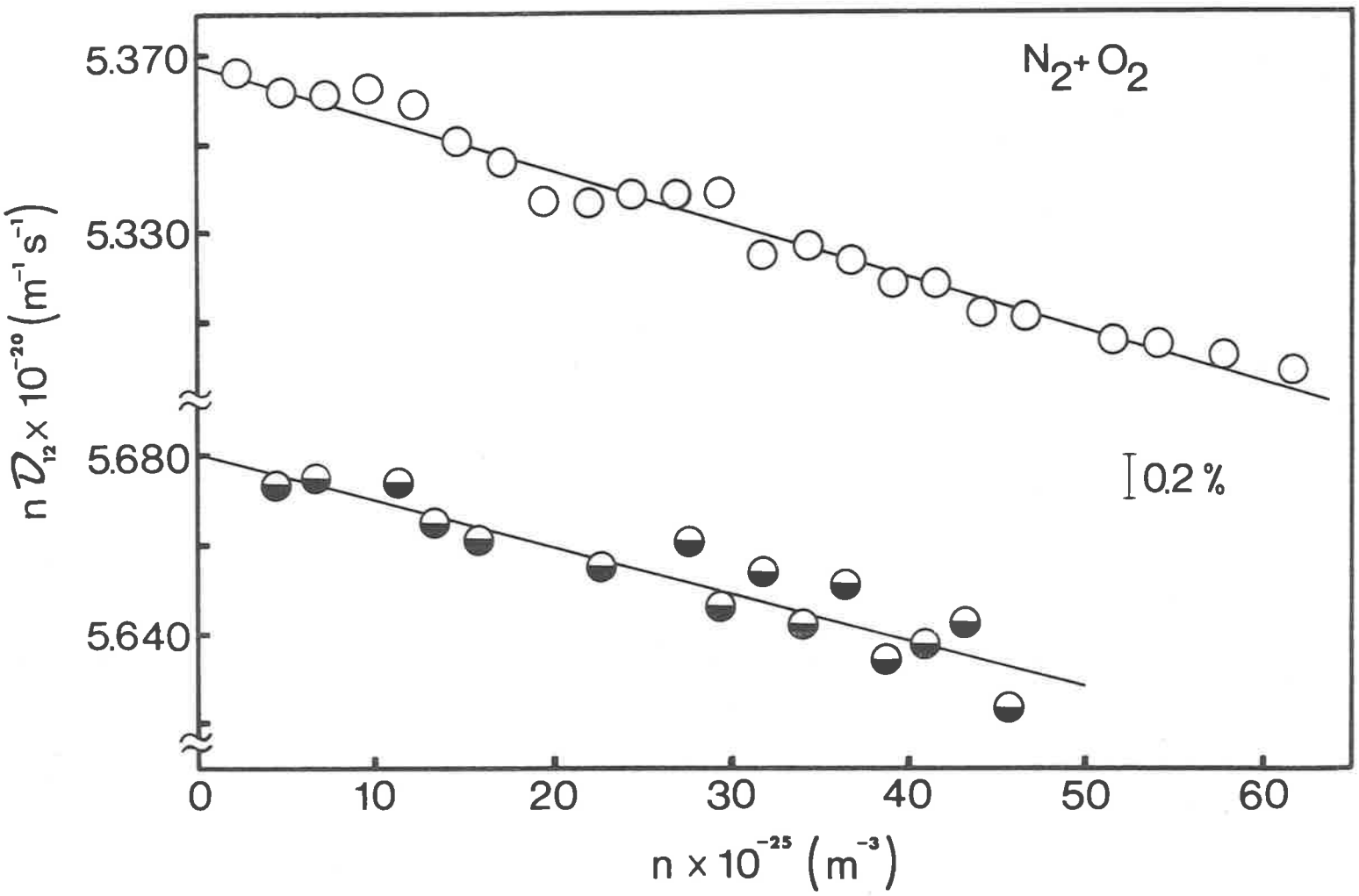

Figure 7.4: Density dependence of $n\mathcal{D}_{12}$ for the $N_2 + O_2$ system; ○, 300.00K, ◒, 323.16K. Multiplicate points are not indicated in the Figure.

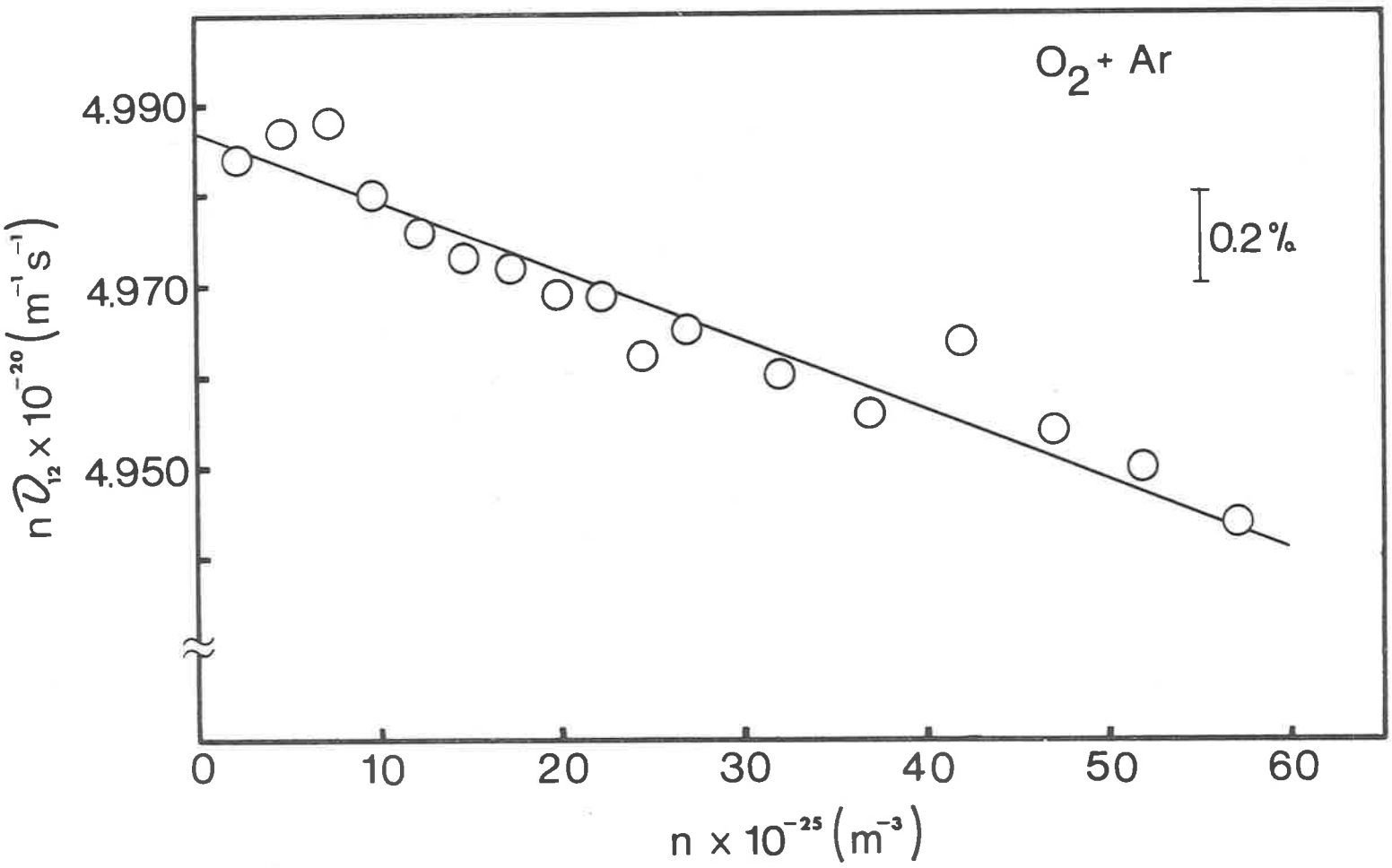

Figure 7.5: Density dependence of $n\mathcal{D}_{12}$ for the O_2 + Ar system; ○, 300.00K. Multiplicate points are not indicated in the Figure.

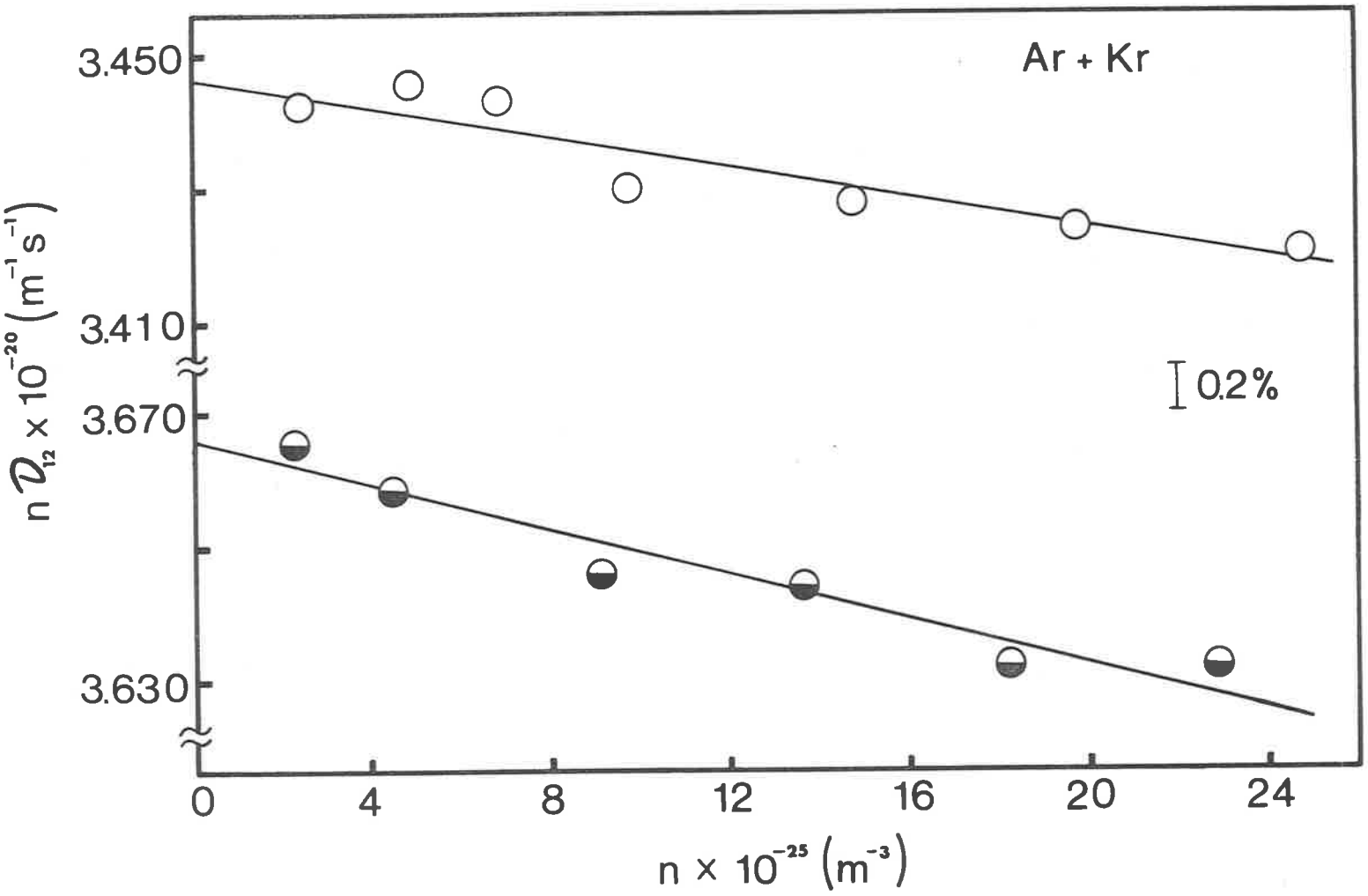

Figure 7.6: Density dependence of $n\mathcal{D}_{12}$ for the Ar + Kr system; ○ , 300.00K, ◒ , 323.16K. Multiplicate points are not indicated in the Figure.

Equations of higher order in n and P were considered, but no significant improvement in the standard deviation of the fit was observed. In addition, the coefficients of n^2 and P^2 were insignificant in comparison with their standard deviations.

The Ar + Kr system was studied only to a pressure of 10 atmospheres for two reasons, firstly, lack of sufficient krypton and secondly, the results of experiments at higher pressures would probably be inaccurate due to the larger value of B_E for this system. With regard to the former of these reasons, it should be noted that the procedure employed in admitting gases to the diffusion cell (see §4.3) caused quite large volumes of gas to be wasted.

7.4 Comparison with Enskog-Thorne Theory

In order to compare the experimental B_D values with those predicted by the rigid spheres theory, it is necessary to expand Equation (2.13) as a series in n and make use of the result derived in Appendix I for $(\partial \ell n a_1 / \partial \ell n x_1)_{T,P}$, *viz.*,

$$(\partial \ell n a_1 / \partial \ell n x_1)_{T,P} = 1 - 4x_1 x_2 kTB'_E + \ldots \quad . \qquad (7.5)$$

This yields

$$B_D = - 4x_1 x_2 kTB'_E - \frac{\pi}{6}(x_1 \sigma_{11}^3 \xi_{12} + x_2 \sigma_{22}^3 \xi_{21}), \qquad (7.6)$$

where

$$\xi_{ij} = (\sigma_{ii} + 4\sigma_{jj})/(\sigma_{ii} + \sigma_{jj}) \quad (i \neq j) \quad . \qquad (7.7)$$

Now, if the rigid spheres expression for the second virial coefficient[2]:

$$B'_{ij} = \frac{2}{3}\pi\sigma_{ij}^3 /kT \quad , \tag{7.8}$$

is employed to evaluate B'_E, then

$$B_D^{RS} = \pi x_1 x_2 (\sigma_{11} - \sigma_{22})^2 (\sigma_{11} + \sigma_{22}) - \frac{\pi}{6}(x_1 \sigma_{11}^3 \xi_{12} + x_2 \sigma_{22}^3 \xi_{21}) , \tag{7.9}$$

where B_D^{RS} denotes the first density correction for the rigid spheres model.

Calculations of B_D^{RS} cannot be performed until some estimation of σ_{11} and σ_{22} is made; for this purpose, a scheme which involved identifying the dilute gas diffusion coefficient with that of a gas composed of rigid spheres was adopted. In other words, the first approximation to the *rigid spheres diffusion coefficient*, which is defined as[2]

$$P[D_{12}]_1^{RS} = 0.002628[T^3 (M_1 + M_2)/2M_1 M_2]^{\frac{1}{2}} \sigma_{12}^{-2} \quad , \tag{7.10}$$

was equated with $(PD_{12})_0$. In this manner, values of σ_{12} were obtained for the N_2 + Ar, N_2 + O_2 and O_2 + Ar systems. Each of these quantities can be related to the particular σ_{11} and σ_{22} by

$$\sigma_{12} = \tfrac{1}{2}(\sigma_{11} + \sigma_{22}) \quad . \tag{7.11}$$

Hence, it is possible to derive a set of three linear equations involving the three σ_{ii} for N_2, O_2 and Ar. The solution of this set of equations is given in Table 7.7; this table also includes a value of σ_{ii} for Kr which could be calculated using Equations (7.10) and (7.11) once the Ar value had been determined.

Table 7.7

Rigid Spheres Diameters from $(P\mathcal{D}_{12})_0$ *Data*

Gas	300.00K σ_{ii} (nm)	323.16K[a] σ_{ii} (nm)
N_2	0.3441	0.3411
O_2	0.3311	0.3275
Ar	0.3394	0.3358
Kr	0.3876	0.3814

[a] For the O_2 + Ar system at this temperature[3], $(P\mathcal{D}_{12})_0$ = 0.2329 atm $cm^2 s^{-1}$ was used for these calculations.

Substitution of these σ_{ii} data into Equation (7.9) yields the B_D^{RS} results listed in Table 7.8; the experimental B_D values are repeated in this table for comparison.

It can be seen that the agreement between B_D and B_D^{RS} is very poor; at best the rigid spheres model predicts the correct sign for B_D and mirrors the larger magnitude of B_D in the Ar + Kr system.

7.5 Modified Enskog Theory

The Modified Enskog Theory (MET) is an empirical extension of the rigid spheres theory to account for the real nature of fluids. It was first proposed by Enskog[4]

Table 7.8

B_D^{RS} *Calculations*

System	T (K)	10^{29} B_D^{RS} (m^3)	10^{29} B_D (m^3)
N_2 + Ar	300.00	- 5.22	- 2.08
	323.16	- 5.07	- 2.00
N_2 + O_2	300.00	- 5.03	- 2.22
	323.16	- 4.88	- 1.85
O_2 + Ar	300.00	- 4.93	- 1.53
Ar + Kr	300.00	- 6.19	- 3.31
	323.16	- 5.95	- 4.54

and has been used with relative success[5-8] in predicting the behaviour of the coefficients of viscosity and thermal conductivity to quite large densities.

Basically, the modification consists of replacing the pressure in the rigid spheres equation of state (Equation (2.7)) with the thermal pressure, $T(\partial P/\partial T)_{\tilde{V}}$, that is[2,9]

$$\frac{\tilde{V}}{R}\left(\frac{\partial P}{\partial T}\right)_{\tilde{V}} = 1 + \frac{b_0}{\tilde{V}} Y , \qquad (7.12)$$

where

$$b_0 = \frac{2}{3}\pi N_0 \sigma_{ii}^3 .$$

This substitution is rigorous for a gas composed of rigid spherical molecules as the internal pressure, $(\partial\tilde{U}/\partial\tilde{V})_T$, is zero. For real fluids the quantity $(\tilde{V}/R)(\partial P/\partial T)_{\tilde{V}}$ in Equation (7.12) can be evaluated using the experimental

equation of state data; for example, if the virial expansion is employed, then

$$\frac{\tilde{V}}{R}\left(\frac{\partial P}{\partial T}\right)_{\tilde{V}} = 1 + \frac{1}{\tilde{V}}\left(B + T\frac{dB}{dT}\right) + \frac{1}{\tilde{V}^2}\left(C + T\frac{dC}{dT}\right) + \ldots . \quad (7.14)$$

Combination of Equations (7.12) and (7.14) yields

$$b_0 Y/\tilde{V} = \frac{1}{\tilde{V}}\left(B + T\frac{dB}{dT}\right) + \frac{1}{\tilde{V}^2}\left(C + T\frac{dC}{dT}\right) + \ldots . \quad (7.15)$$

Now, as the transport coefficients must approach the dilute gas values in the low density limit, it is possible to write[2]

$$b_0 = B_{ii} + T(dB_{ii}/dT) . \quad (7.16)$$

Therefore, an *effective* rigid sphere diameter, σ_{ii}^{EFF}, can be calculated for each temperature according to

$$\sigma_{ii}^{EFF} = (3b_0/2\pi N_0)^{1/3} . \quad (7.17)$$

The results of such calculations are summarised in Table 7.9. An estimation of the uncertainty in σ_{ii}^{EFF}, deduced from the error[1] in B_{ii}, is also given.

In computing the corresponding B_D^{MET} values it is logical to include the *real* activity factor as derived from experimental B_E' data. Inspection of Table 7.10 again reveals a significant discrepancy between the measured B_D and the predicted B_D^{MET} values.

The disparity between B_D and B_D^{MET} for the present systems is *much* worse than that reported previously[10,11] for a number of binary systems containing helium. As suggested by Arora and Dunlop[12], this difference can be explained by

Table 7.9

Effective Rigid Spheres Diameters

Gas	300.00K σ_{ii}^{EFF} (nm)	323.16K σ_{ii}^{EFF} (nm)
N_2	0.352(±0.03)	0.348(±0.03)
O_2	0.322(±0.03)	0.331(±0.03)
Ar	0.334(±0.03)	0.330(±0.03)
Kr	0.378(±0.02)	0.375(±0.02)

Table 7.10[a]

Comparison of B_D *and* B_D^{MET}

System	T (K)	10^{29} B_D^{MET} (m^3)	10^{29} B_D (m^3)
N_2 + Ar	300.00	-5.18±0.2	-2.08±0.1
	323.16	-5.06±0.2	-2.00±0.2
N_2 + O_2	300.00	-5.05±0.2	-2.22±0.2
	323.16	-5.25±0.2	-1.85±0.2
O_2 + Ar	300.00	-4.87±0.2	-1.53±0.3
Ar + Kr	300.00	-6.68±0.1	-3.31±1.3
	323.16	-6.29±0.1	-4.54±1.4

[a] Error in calculation of B_D^{MET} estimated from the uncertainty in σ_{ii}^{EFF} and B_E' .

expressing Equation (7.6) in the form

$$B_D = B_D^a + B_D^T \quad , \tag{7.18}$$

where the activity contribution to B_D is given by

$$B_D^a = - 4x_1 x_2 kTB_E' \quad , \tag{7.19a}$$

and the Thorne expression for the kinetic contribution is

$$B_D^T = - \frac{\pi}{6}(x_1 \sigma_{11}^3 \xi_{12} + x_2 \sigma_{22}^3 \xi_{21}) . \tag{7.19b}$$

If the measured B_D and B_D^a are denoted by $(B_D^a)_{exp}$ and $(B_D)_{exp}$, then an experimental quantity $(B_D^T)_{exp}$ can be derived from

$$(B_D^T)_{exp} = (B_D)_{exp} - (B_D^a)_{exp} , \tag{7.20}$$

and compared directly with calculations based on Equation (7.19b). This type of correlation yields no extra information for the systems studied here because the $(B_D^a)_{exp}$ values are quite small in magnitude. However, for the systems containing helium, $(B_D^a)_{exp}$ generally contributes to the extent of 50% or more to $(B_D)_{exp}$; hence the reason why the MET results are found to agree with $(B_D)_{exp}$ to better than ±10%. In contrast, the disagreement between $(B_D^T)_{exp}$ and B_D^T is conspicuous.[12]

The failure of the Enskog-Thorne theory and its empirical extension is not surprising when the simplicity of the rigid sphere model is considered. Of the assumptions inherent in the theory, neglection of the following are most questionable: ternary and higher order collisions, attractive intermolecular forces, and velocity correlations. Although some attempts to

account for the first two of these phenomena have been reported[13-15] the results are only applicable to single component systems or binary systems at trace concentrations. It is also unfortunate that the theoretical expressions of Bennett and Curtiss[16] which partially account for the effects of three-body collisions have not been numerically evaluated for binary systems.

7.6 *Temperature Dependence of* B_D

One of the other aims of this project was to investigate the temperature dependence of B_D. While it was anticipated that B_D could be measured over the range 275-325K, this did not eventuate because at the lower temperature it proved impossible to align or separate the cell compartments in a time insignificant in relation to the diffusion period. A variety of Apiezon vacuum greases were used in the hope of overcoming the increased friction between the plates, but to no avail. The obvious solution to this problem, namely, releasing the tension in the springs, led to a failure in the ability of the cell to sustain pressures greater than 5 atmospheres. Consequently, experiments were performed at the temperatures 300.00 and 323.16K.

Over this restricted temperature range no *statistically significant* variation in B_D for the N_2 + Ar, N_2 + O_2 and Ar + Kr systems was observed (see Table 7.6). As an initial experiment at 20 atmospheres and 323.16K for O_2 + Ar indicated a similar result, measurements on this system were discontinued. These results cannot be used to imply that B_D is independent of T, but show that a much larger temperature range is necessary before any variation in B_D becomes apparent.

REFERENCES

1. J.H. Dymond and E.B. Smith, *The Virial Coefficients of Gases*, Clarendon Press (1969).

2. J.O. Hirschfelder, C.F. Curtiss and R.B. Bird, *Molecular Theory of Gases and Liquids*, (4th printing), Wiley (1967).

3. H.L. Robjohns and P.J. Dunlop, private communication.

4. S. Chapman and T.G. Cowling, *The Mathematical Theory of Non-uniform Gases*, 3rd edition, Cambridge University Press (1970).

5. J.V. Sengers, *Int. J. Heat Mass Transfer* 8 1103 (1965).

6. H.J.M. Hanley, R.D. McCarty and E.G.D. Cohen, *Physica* 60 322 (1972).

7. J.F. Ely and D.A. McQuarrie, *J . Chem. Phys.* 60 4105 (1974).

8. R. Di Pippo, J.R. Dorfman, J. Kestin, H.E. Khalifa and E.A. Mason, *Physica* 86A 205 (1977).

9. A. Michels and R.O. Gibson, *Proc. Roy. Soc.* A134 288 (1931).

10. G.R. Staker and P.J. Dunlop, *Chem Phys. Letters* 42 419 (1976).

11. T.N. Bell, I.R. Shankland and P.J. Dunlop, *ibid.* 45 445 (1977).

12. P.S. Arora and P.J. Dunlop, to be published.

13. D.E. Stogryn and J.O. Hirschfelder, *J. Chem. Phys.* 31 1531, 1545 (1959).

14. S.K. Kim and J. Ross, *ibid.* 42 263 (1965).

15. W.A. Wakeham, *J. Phys. B: Atom. Molec. Phys.* 6 372 (1973).

16. D.E. Bennett III and C.F. Curtiss, *J. Chem. Phys.* 51 2811 (1969).

APPENDIX I

Thermodynamic Relationships

(i) Activity factor, $(\partial \ell n a_1 / \partial \ell n x_1)_{T,P}$

If the virial equation of state is used to describe a binary gas mixture then the Gibbs free energy, G, of the mixture is given by[1]

$$G = \sum_{i=1}^{2} \nu_i \mu_i^0 + RT \sum_{i=1}^{2} \nu_i \ell n x_i + RT \sum_{i=1}^{2} \nu_i \ell n (P/P_0) + \\ + \sum_{i=1}^{2} \nu_i B_m P + \frac{1}{2RT} \sum_{i=1}^{2} \nu_i (C_m - B_m^2) P^2 + \ldots . \qquad (I.1)$$

Here ν_i denotes the number of moles of component i; μ_i^0 the chemical potential of i in its standard state; P_0 the standard pressure; B_m and C_m the second and third volume virial coefficients of the mixture. C_m is defined in an analogous manner to B_m, *viz.*,

$$C_m = \sum_{i=1}^{2} \sum_{j=1}^{2} \sum_{k=1}^{2} x_i x_j x_k C_{ijk} . \qquad (I.2)$$

Equation (I.1) can be expressed in terms of the pressure virial coefficients as

$$G = \sum_{i=1}^{2} \nu_i \mu_i^0 + RT \sum_{i=1}^{2} \nu_i \ell n x_i + RT \sum_{i=1}^{2} \nu_i \ell n (P/P_0) + \\ + RT \sum_{i=1}^{2} \nu_i B'_m P + \tfrac{1}{2} RT \sum_{i=1}^{2} \nu_i C'_m P^2 + \ldots . \qquad (I.3)$$

The chemical potential of component i, μ_i, can be obtained from the above equation by differentiation with respect to ν_i at constant T, P and $\nu_{j \neq i}$, that is

$$\mu_i = \mu_i^0 + RT\ell nx_i + RT\ell n(P/P_0) + RT\left[2\sum_{j=1}^{2} x_j B'_{ij} - B'_m\right]P +$$

$$+ \tfrac{1}{2}RT\left[3\sum_{j=1}^{2}\sum_{k=1}^{2} x_j x_k C'_{ijk} - 2C'_m\right]P^2 + \ldots \quad . \qquad (I.4)$$

With reference to component 1, rearrangement of this equation gives

$$\mu_1 = \mu_1^0 + RT\ell nx_1 + RT\ell n(P/P_0) + RT\left[B'_{11} + 2x_2^2 B'_E\right]P +$$

$$+ \tfrac{1}{2}RT\left[C'_{111} + 3x_2^2(2C'_{E1} - C'_{E2}) + 6x_2^3(C'_{E2} - C'_{E1})\right]P^2 + \ldots , \qquad (I.5)$$

where

$$B'_E = B'_{12} - \frac{1}{2}(B'_{11} + B'_{22}), \qquad (I.6a)$$

$$C'_{E1} = C'_{112} - \frac{1}{3}(2C'_{111} + C'_{222}), \qquad (I.6b)$$

$$C'_{E2} = C'_{122} - \frac{1}{3}(C'_{111} + 2C'_{222}). \qquad (I.6c)$$

Therefore the logarithm of the activity of component 1, ℓna_1, is

$$\ell na_1 = \ell na_1^0 + \ell nx_1 + \ell n(P/P_0) + \left[B'_{11} + 2x_2^2 B'_E\right]P +$$

$$+ \tfrac{1}{2}\left[C'_{111} + 3x_2^2(2C'_{E1} - C'_{E2}) + 6x_2^3(C'_{E2} - C'_{E1})\right]P^2 + \ldots , \qquad (I.7)$$

where a_1^0 is the activity of 1 in the standard state. Differentiation of ℓna_1 with respect to ℓnx_1 yields

$$(\partial \ell n a_1 / \partial \ell n x_1)_{T,P} = 1 - 4x_1 x_2 B'_E P + \\ - 3x_1 x_2 \left[(3x_1 - 1) C'_{E1} + (3x_2 - 1) C'_{E2} \right] P^2 + \ldots , \tag{I.8}$$

which is the required relationship.

(ii) Concentration dependence of $\bar{V}_1$

An expression for the partial molar volume of species 1, $\bar{V}_1$, in a binary mixture can be obtained from Equation (I.5) using the well known relationship:

$$(\partial \mu_1 / \partial P)_{T,\nu_i} = (\partial V / \partial \nu_1)_{T,P,\nu_2} = \bar{V}_1 . \tag{I.9}$$

Hence

$$\bar{V}_1 = \frac{RT}{P} \Big\{ 1 + \left[B'_{11} + 2x_2^2 B'_E \right] P + \\ + \left[C'_{111} + 3x_2^2 (2C'_{E1} - C'_{E2}) + 6x_2^3 (C'_{E2} - C'_{E1}) \right] P^2 + \ldots \Big\} . \tag{I.10}$$

It follows that

$$(\partial \bar{V}_1 / \partial x_1)_{T,P} = - 4x_2 RTB'_E + \\ - 6x_2 RT \left[(3x_1 - 1) C'_{E1} + (3x_2 - 1) C_{E2} \right] P + \ldots . \tag{I.11}$$

Considering only the first term of this expression, that is

$$(\partial \bar{V}_1 / \partial x_1)_{T,P} = - 4x_2 B_E , \tag{I.12}$$

which when combined with

$$(\partial x_1 / \partial C_1)_{T,P} = 1/(C_1 + C_2)^2 \bar{V}_2 , \tag{I.13}$$

yields

$$(\partial \bar{V}_1 / \partial C_1)_{T,P} = - 4x_2 B_E / (C_1 + C_2)^2 \bar{V}_2 \quad . \tag{I.14}$$

Therefore

$$(\partial \bar{V}_1 / \partial C_1)_{T,P} = - 4C_2 B_E / C^3 \bar{V}_2 \quad , \tag{I.15}$$

where

$$C = C_1 + C_2 \quad . \tag{I.16}$$

(iii) Pressure-of-mixing, ΔP_{mix}

Consider a Loschmidt cell consisting of two compartments with identical volumes V ; each compartment initially contains a binary gas mixture, composed of the same species, at pressure P. If x_u and x_ℓ denote the molefractions of component 1 in the upper and lower compartments respectively, then the total number of moles of gas in the cell is given by

$$\nu_{tot} = (PV/RT)[z_u^{-1} + z_\ell^{-1}] \quad . \tag{I.17}$$

After complete mixing has occurred, the total number of moles is

$$\nu_{tot}^{mix} = 2P_m V / z_m RT, \tag{I.18}$$

where P_m is the pressure at equilibrium.
Equating ν_{tot} and ν_{tot}^{mix} yields

$$P_m / P = \zeta (1 - \zeta B'_m P)^{-1} \quad , \tag{I.19}$$

where

$$\zeta = \tfrac{1}{2}(z_u^{-1} + z_\ell^{-1}) . \tag{I.20}$$

A Taylor series expansion of P_m/P in P gives

$$P_m/P = 1 + [B'_m - \tfrac{1}{2}(B'_u + B'_\ell)]P + \ldots \quad . \tag{I.21}$$

Now, if the molefraction of the mixture is approximated by

$$x_m = \tfrac{1}{2}(x_u + x_\ell) \quad , \tag{I.22}$$

then

$$\Delta P_{mix}/P = \tfrac{1}{2}(\Delta x)^2 \; B'_E \; P + \ldots \quad , \tag{I.23}$$

where

$$\Delta P_{mix} = P_m - P \quad , \tag{I.24a}$$

and

$$\Delta x = x_u - x_\ell \quad . \tag{I.24b}$$

REFERENCES

1. A.D. Buckingham, *The Laws and Applications of Thermodynamics*, Pergamon Press (1964).

APPENDIX II

Mixing Time Estimation

Upon separation of the cell compartments at time t_{opt}, the concentration distribution is given by Equations (3.23) with $b = \ell/2$, *viz.*,

$$C_1(z,t_{opt}) = \bar{C}_1 - \frac{2\Delta C_1}{\pi}[e^{-1}\cos(\pi z/\ell) - \frac{1}{3}e^{-9}\cos(3\pi z/\ell) + \ldots]. \quad (II.1)$$

Now if one considers for example, the isolated lower compartment, then this equation represents the initial concentration distribution in a closed tube with length $\ell/2$. The solution of the diffusion equation in this case is analogous to Equation (3.18) and is of the form

$$x_1(z,t') = \sum_{n=0}^{\infty} A_n \cos(2n\pi z/\ell)\exp(-4n^2\pi^2\mathcal{D}_{12}\, t'/\ell^2). \quad (II.2)$$

Here C_1 has been replaced by x_1 for convenience and the time scale t' is defined by: $t' = 0 \equiv t = t_{opt}$. Forming the difference

$$\delta(t') = x_1(\ell/2,t') - x_1(0,t'), \quad (II.3)$$

and substituting Equation (II.2) gives for large values of t',

$$\delta(t') = -2A_1 \exp(-4\pi^2\mathcal{D}_{12}\, t'/\ell^2). \quad (II.4)$$

To evaluate A_1, Equation (II.1) can be approximated by

$$x_1(z,0) \approx \frac{1}{2} - \frac{2}{\pi} e^{-1} \cos(\pi z/\ell), \qquad \text{(II.5)}$$

and substituted in

$$A_1 = 4/\ell \int_0^{\ell/2} x_1(z,0)\cos(2\pi z/\ell)dz, \qquad \text{(II.6)}$$

(*c.f.* Equation (3.20b)).

Thus

$$\delta(t') \approx \frac{16}{3\pi^2} \exp(-1-4\pi^2 \mathcal{D}_{12} t'/\ell^2). \qquad \text{(II.7)}$$

When $\delta = 0$ the concentration is uniform throughout the compartment; however, a value of 10^{-6} for δ is insignificant in comparison to the uncertainty in the determinations of $\langle x_1^u \rangle$ and $\langle x_1^\ell \rangle$. Therefore if

$$t' \geqslant 3.05(\ell^2/\pi^2 \mathcal{D}_{12}), \qquad \text{(II.8a)}$$

then

$$\delta(t') \leqslant 10^{-6} . \qquad \text{(II.8b)}$$

In other words a period of approximately $3t_{opt}$ is necessary to attain a uniform composition in the cell compartments.

APPENDIX III

Loschmidt Experiment Data

Data relevant to the calculation of $\bar{x}_1$(exp), $P\mathcal{D}_{12}$ and $n\mathcal{D}_{12}$ are summarised in the following tables. Second virial coefficient data necessary for such calculations are given in Tables III.1 and III.2; literature from which the virial coefficients are taken is cited in these tables. Actual experimental results are contained in Tables III.3-9.

All symbols have been defined in the text but are repeated here for convenience.

Cl	:	Loschmidt cell of length 122.83 cm.
C2	:	Loschmidt cell of length 60.00 cm.
C3	:	Loschmidt cell of length 40.00 cm.
P	:	Pressure (atm).
t	:	Diffusion period(s).
$\langle x_1^u \rangle$	:	Molefraction of component 1 in upper compartment.
$\langle x_1^\ell \rangle$	:	Molefraction of component 1 in lower compartment.
$\bar{x}_1$ (exp)	:	Mean molefraction of component 1 calculated according to Equation (4.13).
$P\mathcal{D}_{12}$	:	Product of pressure and diffusion coefficient (atm cm^2 s^{-1}).
n	:	Number density of mixture at $\bar{x}_1$ ($m^{-3} \times 10^{-25}$).
$n\mathcal{D}_{12}$	:	Product of number density and diffusion coefficient (m^{-1} $s^{-1} \times 10^{-20}$).

Where experiments have been analysed in duplicate the second set of data is denoted by (*).

Table III.1

Second Virial Coefficients for the Pure Gases

Gas	T (K)	$10^4 B'_{ii}$ (atm^{-1})	Reference
N_2	300.00	- 1.70	(1)
	323.16	- 0.10	(1)
O_2	300.00	- 6.30	(1)
	323.16	- 4.32	(1)
Ar	300.00	- 6.34	(1)
	323.16	- 4.22	(1)
Kr	300.00	- 20.5	(1)
	323.16	- 15.8	(1)

Table III.2

Interaction Second Virial Coefficients

System	T (K)	$10^4 B'_{12}$ (atm^{-1})	Reference
N_2+Ar	300.00	- 4.27	(2,3)
	323.16	- 2.26	(2,3)
N_2+O_2	300.00	- 3.94	(4)
	323.16	- 1.93[a]	
O_2+Ar	300.00	- 5.70	(5)
Ar+Kr	300.00	- 11.6	(2)
	323.16	- 8.86	(2)

[a] Estimation based on assuming same temperature dependence as B'_{12} for N_2 + Ar.

Table III.3: Loschmidt Experiment Data for N_2 + Ar at 3000.00K

Cell	P	t	$\langle x_1^u \rangle$	$\langle x_1^\ell \rangle$	$\bar{x}_1$ (exp)	$P\mathcal{D}_{12}$	n	$n\mathcal{D}_{12}$
C1	1.000	7200	0.6556	0.3445	0.5000	0.2034	2.448	4.978
C1	1.000	7200	0.6546	0.3444	0.4995	0.2038	2.448	4.988
C1	1.000	7500	0.6486	0.3505	0.4996	0.2038	2.448	4.987
C1	1.000	7500	0.6484	0.3505	0.4994	0.2039	2.448	4.989
C1	1.000	7500	0.6486	0.3502	0.4994	0.2035	2.448	4.981
C1	1.000	7500	0.6488	0.3502	0.4995	0.2034	2.448	4.978
C1	1.000	7500	0.6490	0.3506	0.4998	0.2037	2.448	4.985
C1	1.000	7500	0.6494	0.3507	0.5000	0.2036	2.448	4.982
C1	1.999	15000	0.6488	0.3505	0.4996	0.2035	4.894	4.983
C1	1.998	15000	0.6484	0.3502	0.4993	0.2034	4.893	4.980
C1	2.999	22500	0.6493	0.3504	0.4998	0.2033	7.347	4.981
C1	2.999	22500	0.6480	0.3500	0.4989	0.2036	7.345	4.987
C1	4.001	29520	0.6512	0.3473	0.4992	0.2032	9.805	4.979
C2	4.001	7140	0.6490	0.3492	0.4991	0.2031	9.805	4.977
C2	5.003	9000	0.6479	0.3501	0.4989	0.2029	12.266	4.973
C1	6.001	45000	0.6482	0.3492	0.4986	0.2030	14.718	4.979
C1(*)	6.001	45000	0.6477	0.3490	0.4983	0.2031	14.718	4.982
C2	6.004	11160	0.6432	0.3551	0.4991	0.2029	14.724	4.976
C1	7.002	52500	0.6490	0.3492	0.4991	0.2027	17.179	4.974

Table III.3 (cont.)

Cell	P	t	$\langle x_1^u \rangle$	$\langle x_1^\ell \rangle$	$\bar{x}_1$ (exp)	$P\mathcal{D}_{12}$	n	$n\mathcal{D}_{12}$
C1(*)	7.002	52500	0.6485	0.3490	0.4987	0.2028	17.179	4.976
C2	8.006	14460	0.6479	0.3503	0.4990	0.2024	19.652	4.967
C1	8.503	63780	0.6488	0.3483	0.4985	0.2020	20.875	4.959
C1(*)	8.503	63780	0.6490	0.3483	0.4986	0.2019	20.875	4.957
C2	9.004	16089	0.6490	0.3478	0.4983	0.2019	22.110	4.958
C2	10.005	18000	0.6485	0.3488	0.4985	0.2017	24.577	4.954
C3	11.008	8820	0.6477	0.3488	0.4981	0.2016	27.052	4.954
C3	12.006	9660	0.6473	0.3493	0.4982	0.2014	29.516	4.952
C3	13.008	10500	0.6470	0.3498	0.4983	0.2015	31.993	4.955
C3	14.011	11100	0.6498	0.3467	0.4981	0.2011	34.474	4.949
C3	15.007	12180	0.6459	0.3499	0.4978	0.2010	36.939	4.949
C3	16.011	12900	0.6472	0.3487	0.4977	0.2008	39.427	4.946
C3	17.011	13740	0.6469	0.3488	0.4977	0.2006	41.906	4.943
C3	18.011	14580	0.6467	0.3489	0.4976	0.2004	44.388	4.939
C3	19.016	15360	0.6473	0.3487	0.4978	0.2004	46.884	4.942
C3	20.007	16500	0.6441	0.3515	0.4976	0.2003	49.347	4.939
C3	21.009	17040	0.6462	0.3483	0.4970	0.1998	51.839	4.931
C3	22.011	17880	0.6459	0.3486	0.4970	0.2000	54.334	4.936
C3	21.965	17820	0.6463	0.3480	0.4969	0.1995	54.220	4.925

Table III.3 (cont.)

Cell	P	t	$\langle x_1^u \rangle$	$\langle x_1^\ell \rangle$	$\bar{x}_1$ (exp)	$P\mathcal{D}_{12}$	n	$n\mathcal{D}_{12}$
C3	22.963	18660	0.6461	0.3481	0.4968	0.1995	56.706	4.925
C3	23.013	18660	0.6468	0.3481	0.4972	0.1995	56.826	4.927
C3	23.960	19440	0.6462	0.3477	0.4967	0.1994	59.192	4.926
C3	24.950	20160	0.6476	0.3476	0.4974	0.1995	61.663	4.931
C3	24.948	20280	0.6464	0.3480	0.4969	0.1993	61.658	4.925

Table III.4: Loschmidt Experiment Data for N_2 + Ar at 323.16K

Cell	P	t	$\langle x_1^u \rangle$	$\langle x_1^\ell \rangle$	$\bar{x}_1$ (exp)	$P\mathcal{D}_{12}$	n	$n\mathcal{D}_{12}$
C1	2.001	13200	0.6488	0.3515	0.5001	0.2326	4.547	5.285
C1	3.001	19860	0.6480	0.3509	0.4994	0.2318	6.821	5.267
C2	5.001	7860	0.6482	0.3496	0.4989	0.2316	11.372	5.265
C2	6.004	9480	0.6478	0.3505	0.4991	0.2316	13.654	5.267
C2	7.005	11040	0.6480	0.3500	0.4989	0.2314	15.935	5.264
C2	8.004	12600	0.6484	0.3498	0.4990	0.2313	18.211	5.263
C2	9.007	14220	0.6485	0.3499	0.4991	0.2307	20.497	5.250
C2	10.003	15780	0.6474	0.3495	0.4984	0.2312	22.769	5.262
C3	11.010	7740	0.6481	0.3497	0.4987	0.2304	25.067	5.245
C3	12.006	8460	0.6472	0.3501	0.4985	0.2308	27.340	5.256
C3	13.004	9180	0.6470	0.3496	0.4981	0.2300	29.618	5.238
C3	14.011	9840	0.6480	0.3489	0.4983	0.2300	31.920	5.241
C3	15.011	10800	0.6436	0.3518	0.4976	0.2298	34.206	5.237
C3	16.007	11280	0.6473	0.3494	0.4982	0.2301	36.483	5.245
C3	17.006	12000	0.6471	0.3492	0.4980	0.2299	38.768	5.240
C3	18.006	12720	0.6469	0.3495	0.4980	0.2301	41.058	5.247
C3	19.007	13500	0.6463	0.3496	0.4978	0.2292	43.348	5.228
C3	20.016	14520	0.6430	0.3529	0.4978	0.2295	45.661	5.236

Table III.5: Loschmidt Experiment Data for N_2 + O_2 at 300.00K

Cell	P	t	$\langle x_1^u \rangle$	$\langle x_1^\ell \rangle$	$\bar{x}_1$ (exp)	$P\mathcal{D}_{12}$	n	$n\mathcal{D}_{12}$
C1	1.000	7260	0.6434	0.3566	0.5000	0.2189	2.448	5.357
C1	1.000	7200	0.6430	0.3552	0.4991	0.2194	2.447	5.370
C1	1.001	7200	0.6432	0.3550	0.4991	0.2194	2.449	5.370
C1	1.000	7380	0.6394	0.3586	0.4990	0.2192	2.448	5.365
C1	1.999	14340	0.6440	0.3543	0.4991	0.2190	4.895	5.363
C1	2.000	14400	0.6435	0.3548	0.4992	0.2189	4.898	5.360
C1	3.000	21240	0.6460	0.3522	0.4991	0.2189	7.348	5.361
C1	4.002	28740	0.6444	0.3545	0.4994	0.2188	9.806	5.362
C1	4.001	28560	0.6451	0.3536	0.4993	0.2189	9.805	5.365
C2	5.002	8340	0.6481	0.3497	0.4989	0.2183	12.262	5.352
C2	5.001	8340	0.6480	0.3502	0.4990	0.2189	12.261	5.366
C2	6.001	10020	0.6479	0.3498	0.4988	0.2183	14.718	5.353
C2	6.003	10020	0.6483	0.3498	0.4990	0.2181	14.721	5.349
C2	7.003	11700	0.6482	0.3495	0.4988	0.2178	17.182	5.343
C2	7.003	11700	0.6478	0.3495	0.4986	0.2180	17.181	5.349
C2	8.004	13380	0.6480	0.3491	0.4985	0.2174	19.646	5.337
C2	8.004	13440	0.6475	0.3499	0.4986	0.2175	19.646	5.337
C2	9.004	15060	0.6479	0.3491	0.4985	0.2174	22.108	5.338
C2	9.003	15120	0.6473	0.3496	0.4983	0.2173	22.107	5.336
C2	10.004	16800	0.6470	0.3494	0.4981	0.2174	24.574	5.339

Table III.5 (cont.)

Cell	P	t	$\langle x_1^u \rangle$	$\langle x_1^\ell \rangle$	$\bar{x}_1$ (exp)	$P\mathcal{D}_{12}$	n	$n\mathcal{D}_{12}$
C2	10.005	16800	0.6474	0.3496	0.4984	0.2173	24.576	5.339
C2	11.004	18480	0.6474	0.3495	0.4984	0.2172	27.040	5.339
C2	12.006	20160	0.6474	0.3494	0.4983	0.2172	29.515	5.340
C2	12.987	21840	0.6470	0.3489	0.4978	0.2167	31.940	5.329
C2	12.988	21840	0.6475	0.3488	0.4980	0.2164	31.943	5.321
C2	13.993	23520	0.6472	0.3489	0.4979	0.2167	34.428	5.331
C2	13.979	23580	0.6472	0.3493	0.4981	0.2164	34.394	5.323
C2	14.979	25200	0.6472	0.3486	0.4978	0.2163	36.869	5.324
C2	15.975	26880	0.6474	0.3484	0.4977	0.2160	39.336	5.319
C2(*)	15.975	26880	0.6474	0.3484	0.4977	0.2160	39.336	5.318
C3	15.977	12000	0.6464	0.3491	0.4976	0.2162	39.341	5.323
C2	16.972	28620	0.6465	0.3483	0.4972	0.2160	41.808	5.321
C2(*)	16.972	28620	0.6464	0.3482	0.4971	0.2159	41.808	5.318
C2	17.972	30360	0.6465	0.3482	0.4972	0.2155	44.289	5.310
C2(*)	17.972	30360	0.6467	0.3485	0.4974	0.2157	44.289	5.314
C2	18.968	32100	0.6461	0.3482	0.4970	0.2154	46.763	5.311
C2(*)	18.968	32100	0.6460	0.3484	0.4970	0.2156	46.763	5.315
C2	18.967	32100	0.6459	0.3482	0.4968	0.2154	46.760	5.311
C2(*)	18.967	32100	0,6465	0.3483	0.4972	0.2153	46.760	5.307

Table III.5 (cont.)

Cell	P	t	$\langle x_1^u \rangle$	$\langle x_1^\ell \rangle$	$\bar{x}_1$ (exp)	$P\mathcal{D}_{12}$	n	$n\mathcal{D}_{12}$
C3	20.965	15780	0.6463	0.3480	0.4969	0.2151	51.728	5.306
C2	21.964	37260	0.6454	0.3478	0.4964	0.2150	54.215	5.308
C2(*)	21.964	37260	0.6460	0.3479	0.4967	0.2148	54.215	5.302
C3	23.455	17640	0.6460	0.3472	0.4964	0.2147	57.930	5.303
C2	24.950	42300	0.6464	0.3475	0.4967	0.2145	61.660	5.301
C2(*)	24.950	42300	0.6463	0.3474	0.4966	0.2144	61.660	5.297

Table III.6: Loschmidt Experiment Data for N_2 + O_2 at 323.16K

Cell	P	t	$\langle x_1^u \rangle$	$\langle x_1^\ell \rangle$	$\bar{x}_1$ (exp)	$P\mathcal{D}_{12}$	n	$n\mathcal{D}_{12}$
C1	2.001	12240	0.6484	0.3503	0.4993	0.2497	4.546	5.673
C1	3.002	18360	0.6483	0.3501	0.4992	0.2497	6.822	5.674
C2	5.003	7380	0.6466	0.3514	0.4990	0.2495	11.377	5.674
C2	6.002	8820	0.6473	0.3505	0.4989	0.2491	13.651	5.665
C2	7.003	10260	0.6481	0.3500	0.4990	0.2489	15.930	5.662
C2	10.004	14880	0.6456	0.3515	0.4985	0.2484	22.772	5.654
C3	11.005	7200	0.6477	0.3498	0.4987	0.2480	25.057	5.647
C3	12.005	7860	0.6471	0.3502	0.4985	0.2486	27.340	5.661
C3	13.003	8520	0.6469	0.3493	0.4980	0.2476	29.619	5.641
C3	14.004	9180	0.6468	0.3498	0.4982	0.2482	31.908	5.654
C3	15.007	10140	0.6423	0.3538	0.4979	0.2476	34.199	5.642
C3	16.006	10500	0.6462	0.3494	0.4976	0.2479	36.483	5.651
C3	17.004	11160	0.6470	0.3491	0.4979	0.2471	38.768	5.634
C3	18.003	11940	0.6448	0.3504	0.4974	0.2472	41.055	5.638
C3	19.003	12480	0.6467	0.3493	0.4978	0.2474	43.343	5.643
C3	20.008	13140	0.6475	0.3488	0.4980	0.2465	45.647	5.623

Table III.7: Loschmidt Experiment Data for O_2 + Ar at 300.00K

Cell	P	t	$\langle x_1^u \rangle$	$\langle x_1^\ell \rangle$	$\bar{x}_1$ (exp)	$P\mathcal{D}_{12}$	n	$n\mathcal{D}_{12}$
C1	1.000	7500	0.6491	0.3505	0.4998	0.2035	2.449	4.982
C1	1.000	7500	0.6491	0.3506	0.4998	0.2035	2.448	4.983
C1	0.999	7500	0.6488	0.3511	0.4999	0.2040	2.447	4.994
C1	2.000	15000	0.6490	0.3505	0.4997	0.2036	4.899	4.987
C1	3.000	22500	0.6489	0.3504	0.4997	0.2035	7.354	4.988
C1	3.000	22500	0.6492	0.3506	0.4999	0.2035	7.354	4.988
C2	4.001	7200	0.6485	0.3510	0.4997	0.2030	9.813	4.980
C2	5.002	8940	0.6498	0.3498	0.4998	0.2028	12.277	4.977
C2	5.003	8940	0.6499	0.3497	0.4998	0.2027	12.280	4.975
C2	6.003	10800	0.6490	0.3506	0.4998	0.2025	14.744	4.973
C2	7.004	12540	0.6500	0.3496	0.4998	0.2021	17.211	4.967
C2	7.005	12540	0.6501	0.3500	0.5001	0.2025	17.214	4.977
C2	8.004	14460	0.6489	0.3510	0.4999	0.2021	19.683	4.969
C3	9.004	7200	0.6496	0.3502	0.4999	0.2019	22.154	4.967
C3	9.007	7200	0.6495	0.3502	0.4998	0.2020	22.162	4.971
C3	10.008	8400	0.6426	0.3572	0.4999	0.2015	24.640	4.962
C3	10.006	8580	0.6398	0.3599	0.4998	0.2009	24.638	4.948
C3	11.005	8880	0.6485	0.3513	0.4999	0.2015	27.113	4.965
C3	13.005	10560	0.6478	0.3518	0.4998	0.2011	32.082	4.960
C3	15.009	12120	0.6493	0.3509	0.5001	0.2007	37.072	4.956

Table III.7 (cont.)

Cell	P	t	$\langle x_1^u \rangle$	$\langle x_1^\ell \rangle$	$\bar{x}_1$ (exp)	$P\mathcal{D}_{12}$	n	$n\mathcal{D}_{12}$
C3	17.010	13680	0.6498	0.3503	0.5001	0.2007	42.069	4.964
C3	19.010	15420	0.6491	0.3511	0.5001	0.2001	47.075	4.954
C3	21.009	17040	0.6491	0.3506	0.4999	0.1996	52.092	4.950
C3	23.007	18720	0.6490	0.3507	0.4998	0.1991	57.119	4.944
C3	25.017	20400	0.6490	0.3506	0.5000	0.1987	62.190	4.939

Table III.8: Loschmidt Experiment Data for Ar + Kr at 300.00K

Cell	P	t	$\langle x_1^u \rangle$	$\langle x_1^\ell \rangle$	$\bar{x}_1$ (exp)	$P\mathcal{D}_{12}$	n	$n\mathcal{D}_{12}$
C1	1.001	10860	0.6495	0.3502	0.4998	0.1404	2.451	3.439
C1	1.000	10860	0.6488	0.3503	0.4995	0.1406	2.450	3.443
C1	1.000	10860	0.6488	0.3504	0.4995	0.1406	2.450	3.446
C1	2.002	20940	0.6550	0.3445	0.4997	0.1404	4.911	3.444
C1	2.002	21780	0.6483	0.3504	0.4993	0.1406	4.910	3.450
C2	4.003	10380	0.6484	0.3479	0.4980	0.1394	9.848	3.430
C2	6.004	15600	0.6487	0.3475	0.4979	0.1390	14.808	3.428
C3	8.003	9240	0.6478	0.3458	0.4965	0.1384	19.794	3.424
C3	10.006	11520	0.6482	0.3442	0.4959	0.1379	24.815	3.421

Table III.9: Loschmidt Experiment Data for Ar + Kr at 323.16K

Cell	P	t	$\langle x_1^u \rangle$	$\langle x_1^\ell \rangle$	$\bar{x}_1$ (exp)	$P\mathcal{D}_{12}$	n	$n\mathcal{D}_{12}$
C1	1.000	9480	0.6485	0.3507	0.4996	0.1614	2.273	3.669
C1	0.999	9480	0.6483	0.3502	0.4992	0.1611	2.272	3.662
C1	2.001	18900	0.6495	0.3493	0.4993	0.1608	4.554	3.659
C1	2.000	18900	0.6491	0.3490	0.4990	0.1606	4.552	3.655
C2	4.000	9060	0.6490	0.3487	0.4987	0.1599	9.122	3.646
C2	6.004	13560	0.6490	0.3472	0.4979	0.1595	13.719	3.644
C3	8.001	8040	0.6491	0.3461	0.4974	0.1586	18.319	3.633
C3	10.004	10020	0.6503	0.3452	0.4975	0.1583	22.953	3.632

REFERENCES

1. J.H. Dymond and E.B. Smith, *The virial coefficients of gases*, Clarendon Press (1969).

2. J. Brewer, *Determination of mixed virial coefficients*, Report No. MRL-2915-C, Air Force Office of Scientific Research, No. 67-2795 (1967).

3. P. Zandbergen and J.J.M. Beenakker, *Physica* 33 343 (1967).

4. R.A. Gorski and J.G. Miller, *J. Am. Chem. Soc.* 75 550 (1953).

5. I.Masson and L.G.F. Dolley, *Proc. Roy. Soc.* 103A 524 (1923).